Short-term Innovative and Exploratory Research Project

ALPHA FOUNDATION FOR THE IMPROVEMENT OF MINE SAFETY AND HEALTH

Final Technical Report

1.0 COVER PAGE

Project Title: Combustion Modeling of Explosive Gas Zones in Longwall Gobs

Grant Number: ASTI14-2

Organization: Colorado School of Mines

Principal Investigator: Gregory Bogin Jr.

Contact Information: Phone: (303) 273-3655 Email: gbogin@mines.edu

Research Period of Performance: 05/02/2014 – 07/31/2015

Acknowledgment/Disclaimer:

This study was sponsored by the Alpha Foundation for the Improvement of Mine Safety and Health, Inc. (ALPHA FOUNDATION). The views, opinions and recommendations expressed herein are solely those of the authors and do not imply any endorsement by the ALPHA FOUNDATION, its Directors and staff.

Table of Contents

2.0 Executive Summary

Several mine fires and explosions, including the disaster at the Upper Big Branch mine in 2010 that caused 29 fatalities, have demonstrated that explosive gases can accumulate and explode within gobs of underground longwall coal mines and expand into the active face areas of the mine. Several studies have been conducted looking at reducing the size of Explosive Gas Zones (EGZs) within the gob using various ventilation schemes. If EGZs explode or burn in a diffusion flame, mine personnel working in active areas may be injured from heat, flame and pressure shock trauma. The ultimate goal of this research was the development of a CFD model of the longwall gob which can simulate EGZs based on various ventilation schemes and includes a combustion model to simulate explosions within the gob to determine the explosion hazard to miners working in the face or bleeder areas surrounding the gobs. Understanding the impact of an explosion in the longwall gob resulting from EGZ formation in the gob can guide new designs for mitigation strategies or containment of an explosion or improve the mine's emergency response and evacuation protocols to increase miners' safety. Currently there are models which can predict location and volume of EGZs in a longwall gob, but are not capable of predicting the impact of explosion on miners if it occurs in the gob or nearby areas. Having a model with this capability would be crucial to mine operators in designing better explosion containments, improved ventilation schemes, and improved response and evacuation protocols.

The specific objectives, approaches, and their relative impact were: 1) Investigate the explosive gas zones (EGZs) in gob-like conditions using an explosion testing apparatus. A gas explosion test facility (GETF) was constructed to study flame propagation through rock rubble with various gob parameters. This study has provided insight into the impact of the conditions found in the gob on explosions and flame propagation providing more accurate parameters to use in developing a combustion model. 2) Development and validation of a CFD combustion model using experimental data obtained from the utilization of an experimental apparatus to study the impact of explosions within a longwall gob. A CFD combustion model of the test apparatus was developed and validated with the results of the physical explosion tests. This validation is critical to gain the explosion propagation, pressure and flame spread parameters that are needed to examine EGZ explosions in longwall gobs. 3) Finally, incorporating the CFD combustion model into the full CFD ventilation model to investigate the safety hazard of EGZs based on methane/air concentrations, volume, location, gob conditions, and effective source of ignition.

The accomplishment of the three tasks led to an improved understanding of the impact of rock rubble on flame propagation. With initial results of the full-scale model predicting a rapid transition (~1 ms) of a turbulent deflagration wave to detonation near and around the shields at the edge of the gob area where the ignition event and EGZ was located, this explosion would result in a major catastrophe. Another investigation of having an ignition event further (2073 m from face) into the gob, resulted in significantly slower growth and no detonation at similar time scales. Results from this exploratory research have shown some very promising results. Determining the specific hazards that miners may face as a consequence of such explosions and safe conditions (distance from face, volume and gas composition) that must be maintained to control the safety hazard from EGZ explosions. Each of the three objectives were interconnected and relied on an iterative approach to finalize a model which was capable of assessing the potential explosion hazard to miners due to the EGZs in the longwall gob. It is expected that this research has the potential to assist in making longwall mines safer by eliminating or, at least, controlling the explosion and fire hazard stemming from EGZs in longwall gobs.

3.0 Problem Statement and Innovation Objective

Summary of Problem statement

Underground longwall coal mining causes the overburden to cave in above the mined-out area called the gob. The caving process causes a large increase in rock permeability, allowing methane stored in the surrounding strata to migrate into the caved area where it can produce an explosion hazard. Explosions in explosive gas zones (EGZs) in longwall gobs and surrounding areas have caused numerous mine disasters and multiple fatalities, as described in detail by Brune (2013) [1]. Examples of recent mine fires and explosions as a result of EGZs in the longwall gob include: 1) The Willow Creek mine explosion and fire in 2000 which fatally injured two miners and injured eight due to multiple explosions possibly caused by a sandstone roof falling and causing ignition of an EGZ in the longwall gob (McKinney et al., 2001) [2]. 2) The Upper Big Branch mine explosion in 2010 resulting in twenty-nine miners being fatally injured (Page et al., 2011) [3]. It was documented by Brune (2013) [1] that, based on numerous past mine explosions and fires, that EGZs exists in most, if not all, longwall gobs.

Several studies have been conducted looking at reducing the size of EGZs within the gob using various ventilation schemes which include:

- Bleederless (progressively sealed) gobs with gob ventilation boreholes to control methane (Balusu et al., 2005). [4]
- Bleeder ventilation studying spontaneous combustion (spon com) to face advance rates (Yuan & Smith, 2010). [5]
- Bleederless operation with nitrogen injection into boreholes or TG location to control spon com (Ren et al., 2012). [6]
- Bleederless operation with nitrogen injection at HG locations to control spon com (Ren et al., 2005; Ren & Balusu, 2009). [7,8]
- Bleederless operation with nitrogen injection at HG locations to control oxygen ingress in multiple panels (Ren et al., 2011). [9]
- Spon com produced gas flow patterns of CO and H2 (Ren & Balusu, 2008). [10]
- Bleederless operation with nitrogen injected at the corner of the HG to control spon com (Yuan & Smith, 2008). [11]

From these studies it appears that neither bleeder ventilation schemes nor progressively sealed, bleederless ventilation is capable of removing 100% of the EGZ across in the gob during all conditions for operation of the longwall mine. Thus, there is a need to provide insight into "what if" scenarios when an explosive gas mixture in the longwall gob is present along with an effective source of ignition causing an explosion near or far from the longwall shields and face area. **Understanding the impact of an explosion in the longwall gob resulting from EGZ formation can guide new designs and mitigation strategies: (1) reducing potential explosive hazards in critical areas, (2) containment of an explosion, (3) and improvement in the mine's emergency response and evacuation protocols to increase miners' safety.**

Research Gaps and Barriers

Current research gaps and barriers preventing a solution include the lack of accurate combustion and explosion models for porous media conditions representative of a rock rubble which can be used to accurately simulate fires and explosions[1] (deflagrations) within the longwall gob. There are two major requirements for a combustion and explosion model to successfully represent an explosion within the longwall gob:

1) A fundamental understanding of flame propagation and explosion behavior in a porous medium similar to the conditions (e.g. permeability, porosity, flow dynamics, gas composition etc…) found in the gob; this requires sufficient experimental data covering a large range of conditions that can be used to develop and validate the model. There have been prior studies investigating basic flame propagation and explosion in a porous media (for instance Mihalik et al., and Bulakov)[12, 13]. However, the majority of these studies lack the actual material properties (e.g. porosity, permeability, conductivity, heat transfer coefficients, etc…) found in various longwall gobs which have shown to have a significant impact on heat transfer and flame propagation within the porous media (Howell et al., 1996)[14]. One of the goals of this work was to provide experimental data of flame propagation through rock rubble under conditions which could simulate a longwall gob. These conditions were utilized to develop and validate a combustion model which was incorporated into a full three dimensional longwall gob model.

2) Knowledge of the physical conditions within the longwall such as methane-air concentrations, flow patterns, pressures and permeability is crucial to developing a successful model. However, this information is not possible to obtain due to the difficulty in accessing the gob region in a longwall coal mine. Thus, the researchers have to rely on numerical models (combination of geo-mechanical and ventilation models) to estimate the conditions in the gob. Recently, researchers at the Colorado School of Mines have developed computational fluid dynamics (CFD) models which allow various ventilation schemes to be modeled; investigating the impact of a chosen ventilation scheme (e.g. bleeder, progressively sealed gob ventilation, nitrogen injection, face ventilation quantity, back return provisions, etc…) on the location and volume of explosive gas zones within the longwall gob (Gilmore et al, 2013 Marts et al., 2013)[15, 16]. Marts et al.[17] have also had success using CFD and FLAC geo-mechanical modeling to provide permeability and porosity parameters of the gob material in three dimensions. This new information about the conditions of the longwall gob along with predicted location and volume of the EGZs was utilized to assist in setting the initial conditions of the experiments for model validations. Ultimately, the CFD model of the longwall gob with the inclusion of the combustion model was able to predict location and volume of the EGZs and predict the potential impact of an explosion in the gob behind the shields.

[1] The term “explosions” used throughout this proposal refers to propagation of deflagration waves only

Innovation Identification and Research Goals

The ultimate goal of this proposed research is the development of a CFD model of the longwall gob which can simulate EGZs based on various ventilation schemes and includes a combustion model to simulate explosions within the gob to determine the explosion hazard to miners. Currently, researchers at CSM have developed a CFD model which can successfully model various ventilation schemes and predicts the explosive gas zones within the longwall gob. However, there was no combustion/explosion model incorporated within this CFD model; which was the motivation for this proposed research. This proposed research allowed for the development and experimental validation of a combustion/explosion model which has been used to simulate explosions within the longwall gob. This full CFD model with ventilation and combustion/explosion model has the potential to allow various mines to fully assess the potential for an explosion hazard and the potential impact an explosion could have on the miners working in the longwall. This model could also provide guidance for improved designs for explosion containment, ventilation, and improved evacuation protocols.

Specific aims and goals

The specific aims for this proposed research was: 1) Investigate the explosive gas zones (EGZs) in gob-like conditions using an explosion testing apparatus. This provided insight into the impact of the conditions found in the gob on explosions and flame propagation providing more accurate parameters to use in developing the combustion model. 2) Development and validation of a CFD combustion model using experimental data obtained from the proposed design of an experimental apparatus to study the impact of explosions within a longwall gob. 3) Finally, incorporating the CFD combustion model into the full CFD ventilation model to investigate the safety hazard of EGZs based on methane/air concentrations, volume, location, gob conditions (e.g. porosity, permeability, moisture, etc..), and effective source of ignition.

Overall, the project was successful in that each of the specific aims proposed were accomplished and several major accomplishments were achieved as well as several new potential areas of future research came about as a result of the discoveries during this 15 month exploratory research program. The specific aims of this research project provided an improved understanding of methane ignition and flame propagation through simulated gob (i.e. rock rubble) as a function of gob conditions across a wide range of physical scales, which ultimately led to the development of a combustion model and fully coupled 3D CFD and combustion model for a longwall coal mine which can begin to provide insight of the consequences of a methane explosion within the gob directly behind the shields which could be a hazard to the miners working in the face and/or bleeder areas surrounding the gob.

Major breakthroughs/innovations initiated by this research effort

1) A successful combustion model of varying methane-air mixtures was developed using a commercially available CFD package. The combustion model has been successfully validated with different size flame reactors. A combustion model which simulates flame propagation through a simulated gob has also been developed, details of the development of this model is provided in section 4.0, along with a summary of results from this model presented below in section 5.0. **The CFD combustion model developed from this funding is the first combustion model which has shown the effects of flame propagation with a simulated gob interface**. The combustion model captures the flame development, transition and propagation as verified in a quartz tube. The combustion model's predicted burning velocity follows the same geometric scaling behavior as measured burning velocities. The model's ability to capture not only the scaling behavior of burning velocities but also the physical structure of the flame as observed in the quartz tube is significant because observation of the dynamic flame structure in a steel tube is not possible. Yet it is important to ensure accurate representation of the methane explosion with the model.

2) **The successful design, fabrication and installation of a small-scale and large-scale flame reactors as part of the newly established Gas Explosion Test Facility, which allows investigation of methane explosions through rock rubble used for combustion model validation along with providing an extensive database for future use in assessing potential methane explosion hazards with a focus on increasing mining safety.** The small-scale test facility consists of two reactors: a 5 cm diameter steel reactor and 13.5 cm diameter quartz reactor. The large-scale test facility consists of two steel reactors: a 31 cm diameter reactor installed in a state-of-the-art research laboratory and a 71cm diameter reactor installed outdoors at CSM's experimental mine research facility. Details of the design, fabrication and installation of the reactors are found in section 4.0.

3) The integration of the combustion model developed has been incorporated into a larger CFD model for a longwall mine with a U-type ventilation system. **This is the first fully coupled three-dimensional CFD and combustion model of a longwall mine which has the ability to predict EGZ and the impact of methane explosions.** These new modeling results provide additional insights into the potential of methane explosions in and around the gob area, preliminary results have been incorporated into a conference paper and submitted to the 2016 SME annual meeting.

Each of the major breakthroughs/innovations and results which are presented in detail in this Final Report has also been converted into three manuscripts; two of which have been submitted for journal publications, and one for preprint to the 2016 SME annual meeting.

4.0 Research Approach

Research Strategy

The formation of EGZs in a longwall gob being documented as the most likely cause of several mine disasters is the current motivation for this proposed research project. Currently, there is no comprehensive model available which can predict location and volume of EGZs in a longwall gob and provide information about the potential hazard of an explosion in the gob. Having a model with this capability would be crucial to mine operators in designing improved ventilation schemes, better explosion seals, and improved emergency response and evacuation protocols.
As discussed earlier, the researchers at CSM have successfully validated a CFD model (ANSYS, 2012)[18] of a longwall gob predicting volume and location of EGZs and have characterized the gob material with respect to permeability and porosity parameters using FLAC (Itasca, 2009)[19]. If the location, volume and gas composition of an EGZ is known, one can numerically model the combustion and flame propagation processes in an explosion and determine whether such explosion will harm miners working in the longwall face and adjacent entries. The impact of an explosion as predicted by a model can help aid experimental testing like those performed by Sapko et al.[20] looking at the impact of explosions on seal design. Specifically, researchers can determine EGZ parameters (e.g. volume, distance from the face, gas composition etc.…) that must be achieved and maintained to keep miners safe.

Innovative elements of this research effort compared to previous research in the field

The innovative element of this research involved the development of a three-dimensional CFD model with an incorporated combustion model capable of predicting a methane explosion in the gob area of a longwall coal mine (more specifically a U-type ventilation). A model capable of this task had not previously been done and with this new innovation comes the ability to study more extensively potential explosion hazards in the longwall mine and various mitigation strategies.

Bulakov (2009)[13] performed experiments investigating the explosion-suppression properties of gob rock with varying rock rubble "lumpiness" and barrier lengths at approximately stoichiometric methane-air conditions. The work did not look at the varying concentrations of methane-air found in the gob as well as varying the material properties of the gob all of which will impact the behavior of the explosion and flame propagation in the rock rubble found in a longwall gob. Also, in many of the case studies reviewed by Brune (2013)[1] diffusion flames formed in EGZs where the methane concentration was above the upper explosive limit. In the Upper Big Branch case, such a diffusion flame may have burned for approximately two minutes (Page et al., 2011)[3], giving miners time to escape before it turned into an explosion. Such cases have not been studied experimentally or with adequate numerical models that can be readily applied to longwall gobs.

Prior CFD modeling of a longwall mine by researchers at CSM had shown a wide variance in the ingress of oxygen into the gob with the variation of the porosity of the gob. This prior work has also predicted the location of EGZ's in the gob based on various ventilation schemes. The location and size of these EGZs provide the initial conditions for simulating explosion events in

the gob area. This current work was innovative in that the researchers were able to take this prior CFD model and incorporate a combustion model developed and validated under various gob parameter , methane-air mixtures, combustion chemistry, and flame dynamics to adequately account for methane explosions in the gob are which could serve a potential hazard to workers in the longwall face.

Research Tasks undertaken with this research effort

Task 1 - Design, Fabrication, and Installation of a small-scale and large-scale Gob Explosion Simulation Apparatus as part of the Gas Explosion Test Facility

In order to develop a large-scale fully coupled CFD and combustion model of methane-air explosions in coal mines, the researchers undertook a strategy of investigating ignition and flame propagation through rock rubble as a function of physical scale experimentally, and used this to inform a simultaneous modeling effort. Originally, the researchers proposed to build just a single large scale apparatus to provide data for validation of the newly developed combustion model. However, it was determined that a more scientific approach of using multiple flame reactors of varying diameters and length was necessary to ensure a robust model was developed which was capable of modeling combustion on the scales of a longwall mine, especially since experiments at this scale was not possible. This new scientific approach of using multiple flame reactors provided insights into how the combustion characteristics changed with scale and whether the newly developed model could capture this effect, which would not have been possible if the original plan of one large reactor was used since it was not at the scale of an actual longwall mine. The small-scale tests provided initial experimental data and guided the test matrix developed for the two reactors that were part of the large-scale testing, allowing for rapid feed-back for model development and installation and safety compliance at the larger scales.

Task 1.1 Design and experimental setup of the two small-scale testing apparatus

Two small scale flame horizontal flame reactors were designed to provide initial investigation of the methane flame propagation and guide experimental matrix of the large-scale test apparatus.

Task 1.1.1 Overview of Steel Flame Reactor Design

A custom design (fabricated in-house) steel flame reactor (5 cm x 1.5 m) with one end open to atmosphere and the other end closed allowing for delivery of a fuel-air mixture, in addition there are four ion sensor ports along the length of the reactor as seen below in Figure 1.

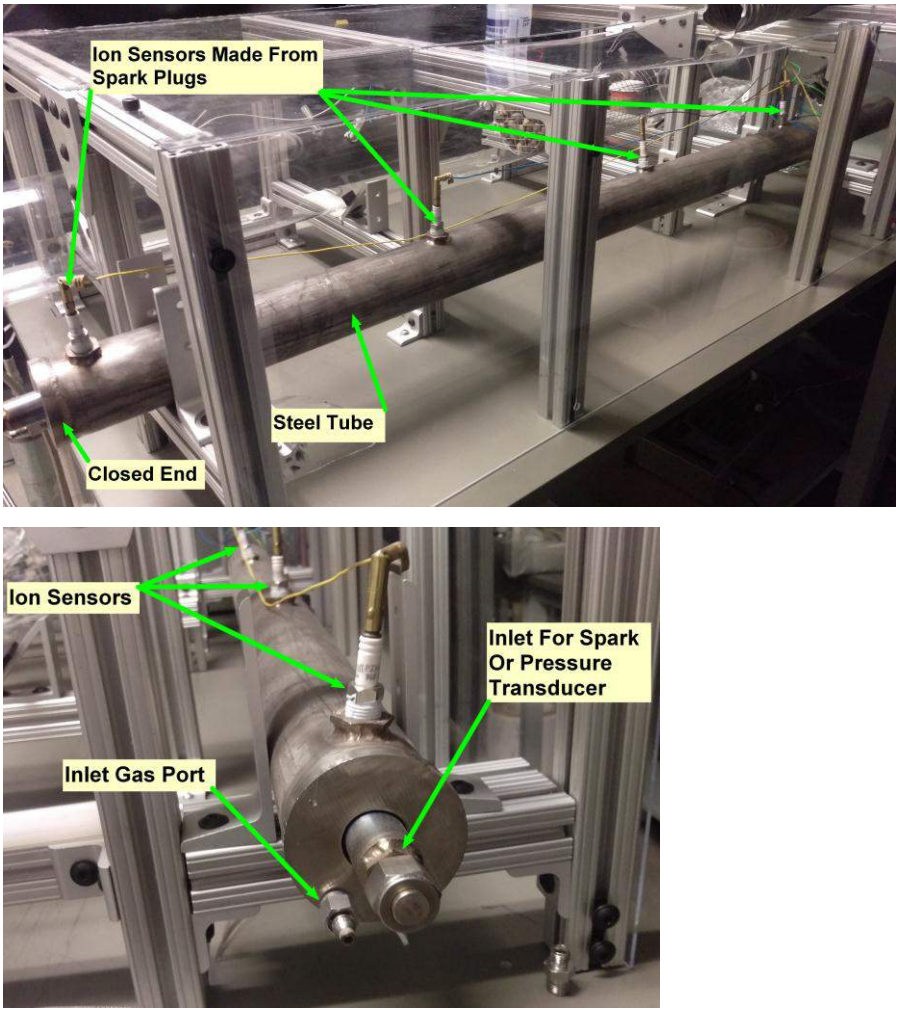

Figure 1. Image of 5 cm steel reactor with various sensor ports .

The steel reactor is made of 0.6 cm thick steel to handle any significant pressure rise. The ports are spaced equally apart at 38 cm along the length of the reactor, they were designed with 10 mm diameter threads to allow standard automotive spark-plugs (converted to ion sensors) to be placed in the sensor ports for ease of measuring flame propagation.

Task 1.1.2 Overview of Quartz Flame Reactor Design

A quartz reactor was designed and fabricated (contracted with outside vendor) to observe and investigate flame propagation, and the dynamic behavior of the flame after ignition as it transitions from a flame kernel to laminar propagating flame and finally to a turbulent flame. The quartz reactor was also designed to have a diameter at least 2 times larger, but have an equal length as the steel reactor discussed above to allow for studying the effects of increasing diameter and volume of explosive gas mixture. CAD drawings and images of the quartz flame reactor is presented below in Figure 2a and 2b.

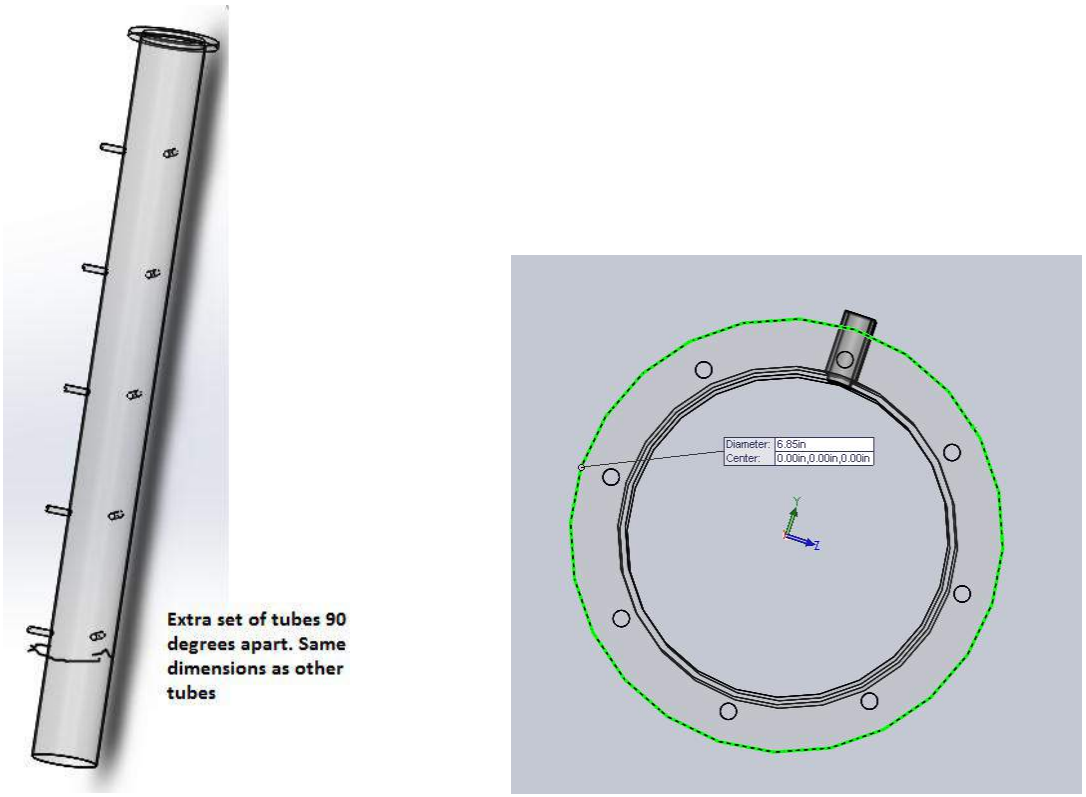

Figure 2a. CAD drawing of the quartz reactor (13.6 cm diameter and 1.5 m length) with ten sensor ports equally spaced 90° apart along the length of the reactor. Full reactor drawing (left image), along with custom flange for fuel-air delivery (right image).

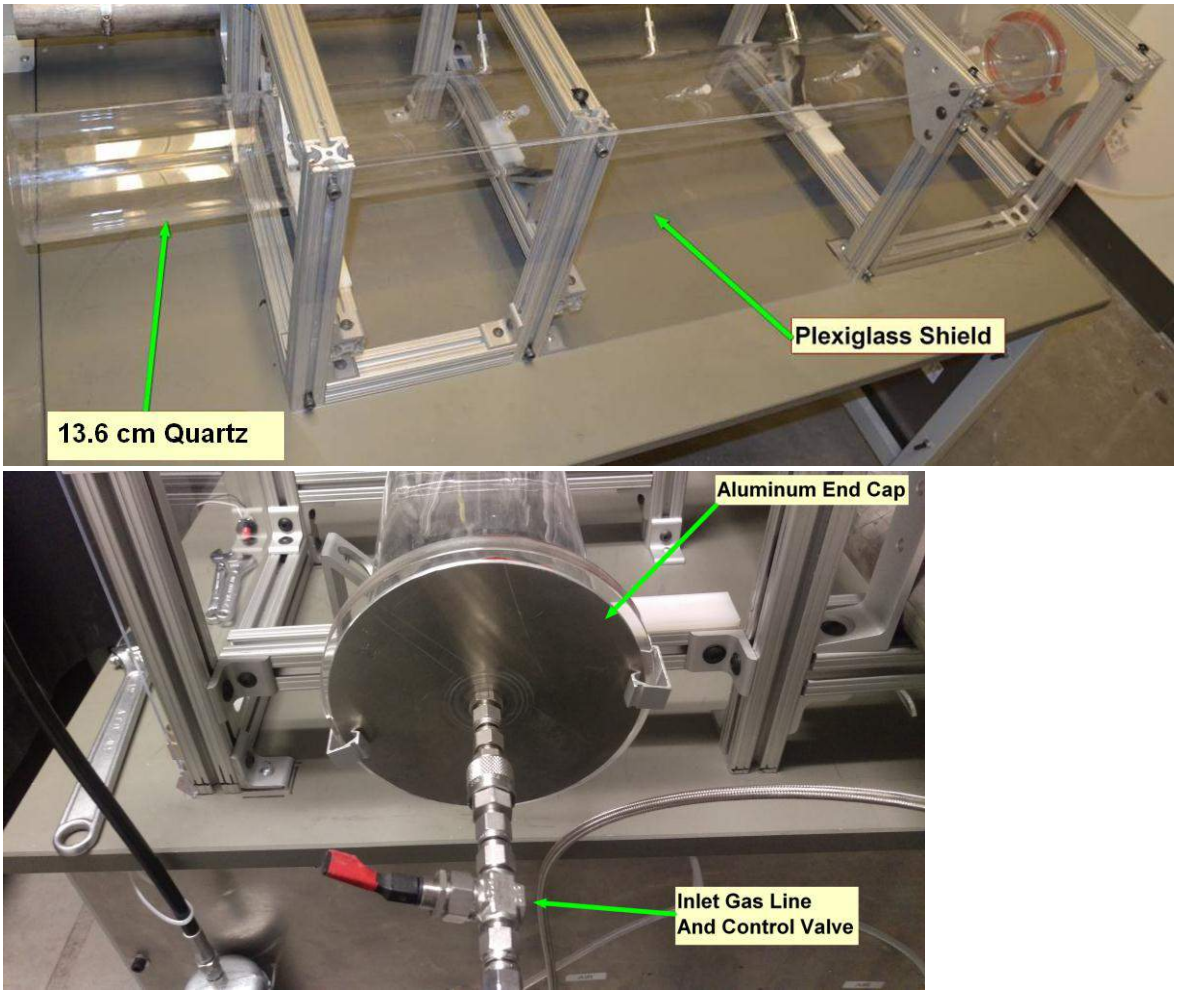

Figure 2b. Image of the quartz reactor (13 cm diameter and 1.5 m length) with ten sensor ports equally spaced 90° apart along the length of the reactor.

The quartz reactor is designed to handle a 1.0 MPa pressure differential. The sensor ports are 1.27 cm in diameter with a height of 2.54 cm extending radially outwards from the flame reactor and are equally spaced 25.4 cm apart along the length of the reactor.

Task 1.1.3 Experimental Setup for the Steel and Quartz flame reactor

A premixed mixture of methane-air fuel are delivered to the closed end of the flame reactors via mass flow controllers which allow the fuel-air ratio to be set based on desired test conditions as seen below in the schematic and image of test apparatus in Figure 3 and Figure 4.

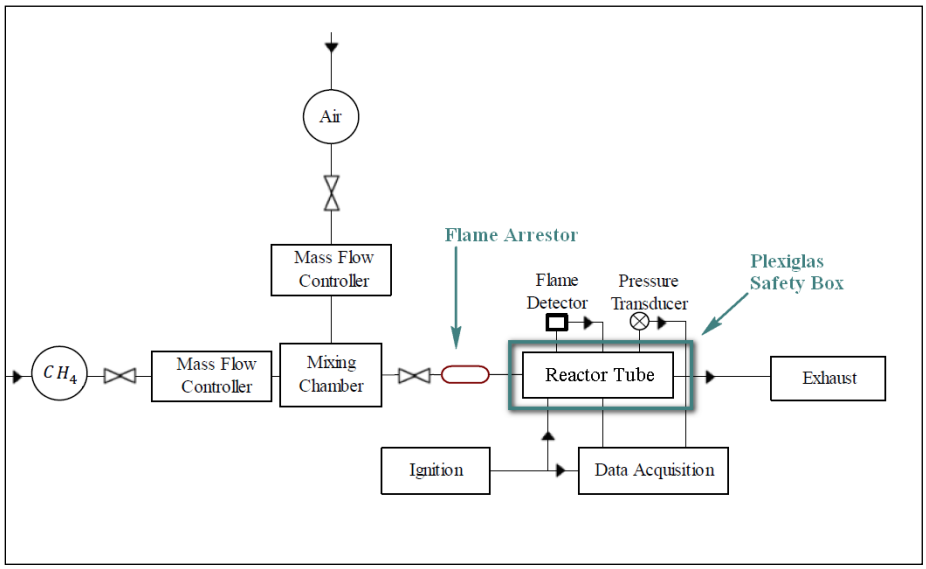

Figure 3. Schematic of the steel and quartz flame reactor.

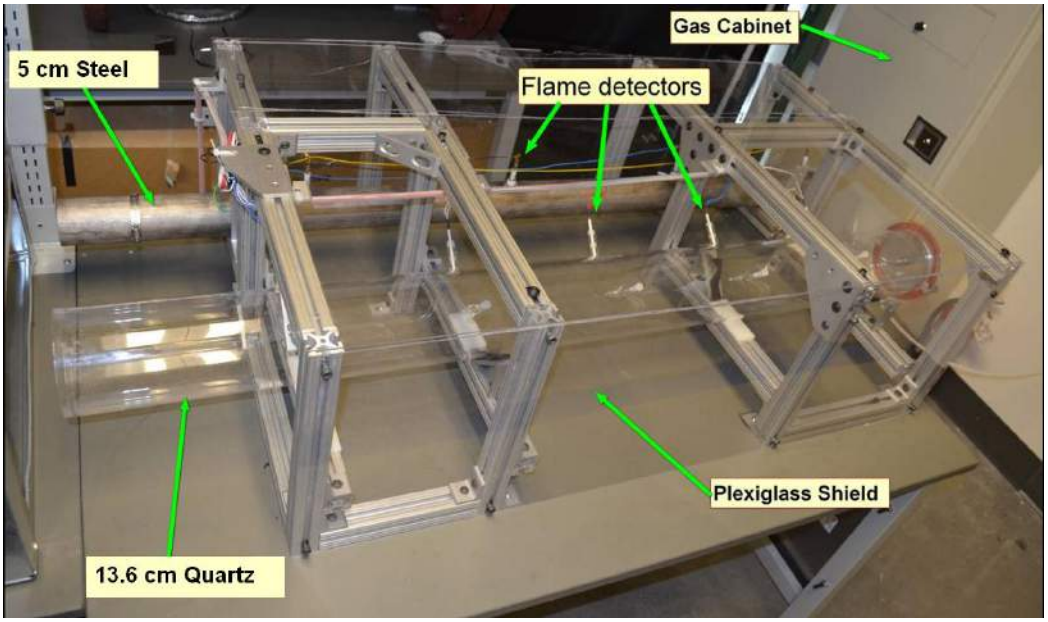

Figure 4. Image of the experimental apparatus for the steel and quartz reactor.

The methane and air are both supplied from high pressure compressed gas cylinders. The flow rates are precisely controlled by separate mass flow controllers, a Sierra Instruments Side-Trak III (0-10 SLM) for the methane and a Teledyne Hastings 200 Series (0-50 SLM) for the air. The MFCs were calibrated before experimental setup, and an Infrared Industries IR-6000 gas analyzer (0-25% CH_4 by vol) was used to determine the actual methane-air mixture delivered to the flame reactors. The methane and air both enter a mixing tank prior to entering the flame reactor. With regards to safety a methane flame arrestor along with nitrogen or air purge system (not shown in schematic above) is utilized after each filling to remove any methane and premixed fuel-air mixture left in the lines between the methane cylinder and the reactor. After each run the flame reactor is purged with compressed air to ensure adequate cooling and the removal of combustion products before the next experiment. The methane-air mixture is ignited using a piezo-electric ignition system. The flame propagation speed along the length of the reactor is determined by custom ion sensors (designed and fabricated in-house) as seen in Figure 5.

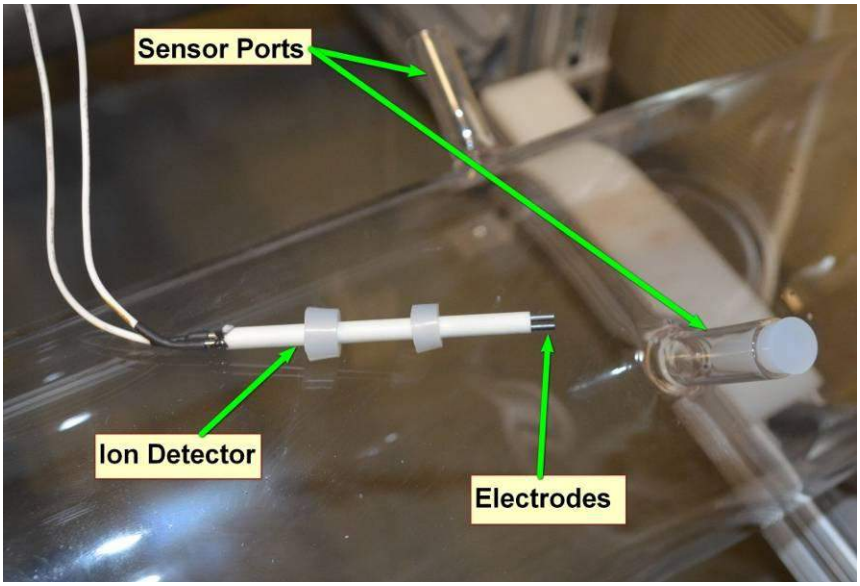

Figure 5. Custom ion sensors as shown for the quartz flame reactor.

The flame detector setup was created by utilizing a DC source to create a potential difference between the electrodes, in effect treating the electrodes like an electrical capacitor. In serial connection with the plug is an electrical resistor. It is the voltage drop across this resistor that gives the measured quantity. When a flame goes near to the gap between the ion sensor electrodes, the accompanying region of ionized particles creates a pathway for the discharge of the stored charge.

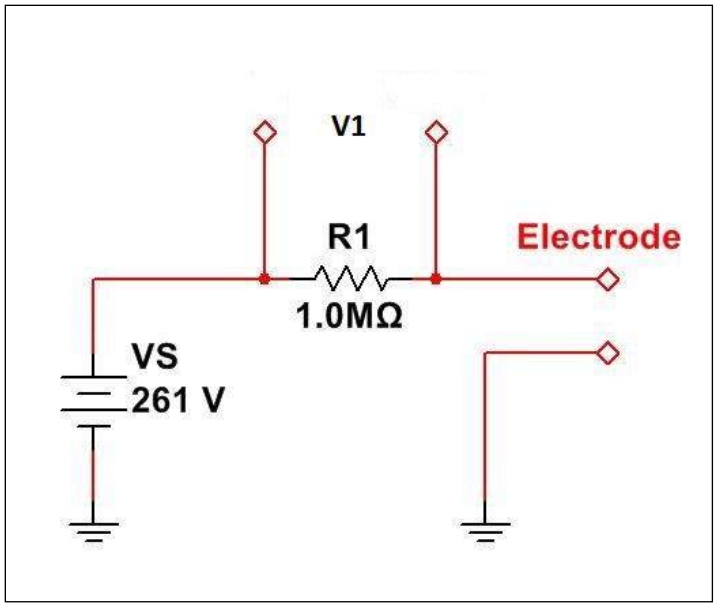

Figure 6. Electrical schematic for a flame detector

This device has been tested and found reliable. A sample signal produced in the laboratory using the current equipment is shown below. Several tests confirmed that the sensor can pick up a passing flame and also a steady flame.

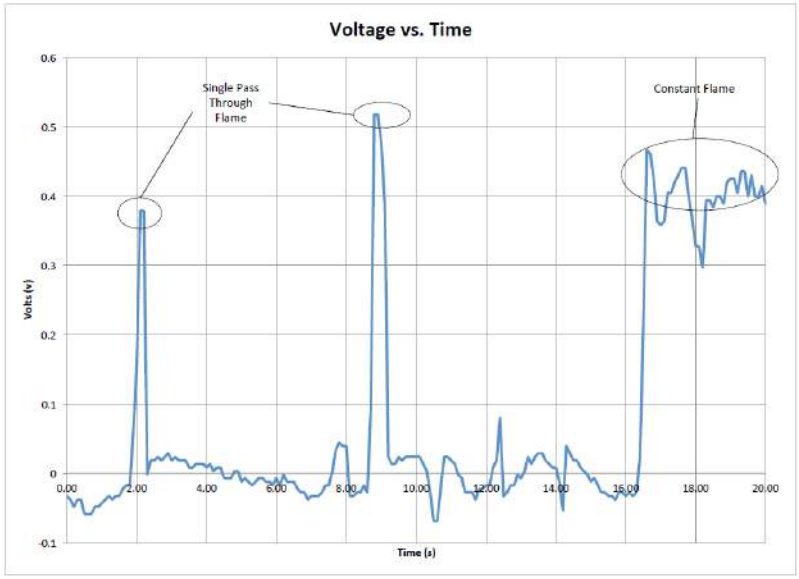

Figure 7. Signal output of the flame detector for transient and steady flame.

The electronic data acquisition is done through a NI cRIO-9075 integrated system, which combines a real-time controller and a reconfigurable and programmable gate array chassis for control and monitoring. This device features a 400 MHz real-time processor and an 4-slot chassis to allow for all the needed measurements. The c-type modules used with the cRIO consist of a 10 V analog NI 9201 input card for the pressure and flame detector signals and a 10 V analog NI 9264 output card. For temperature measurements, the cRIO is equipped with both a 78 mV NI 9213 and also an 80 mV NI 9211 thermocouple input module, which together allow use all common thermocouple types. This ensemble provides more than enough acquisition and control hardware for the current configuration and will accommodate expanded capabilities such as valve control and precise ignition timing.

A portable electronic data acquisition was also designed to allow more efficient setup for indoor and outdoor usage. This system is done through a NI usb-6008 and usb-6009 DAQ boards, which allow for up to 48000 samples per second - high enough to capture the passing of the flame. This ensemble provides more than enough acquisition and control hardware.

An example signal from the ion sensors along the length of the quartz flame reactor is shown in Figure 8. The black peak indicates the flame near the open end of the tube just after the ignition event. Addition voltage spikes (FD 2, FD3 ...) represent the remaining four ion sensors along the length of reactor towards the closed end.

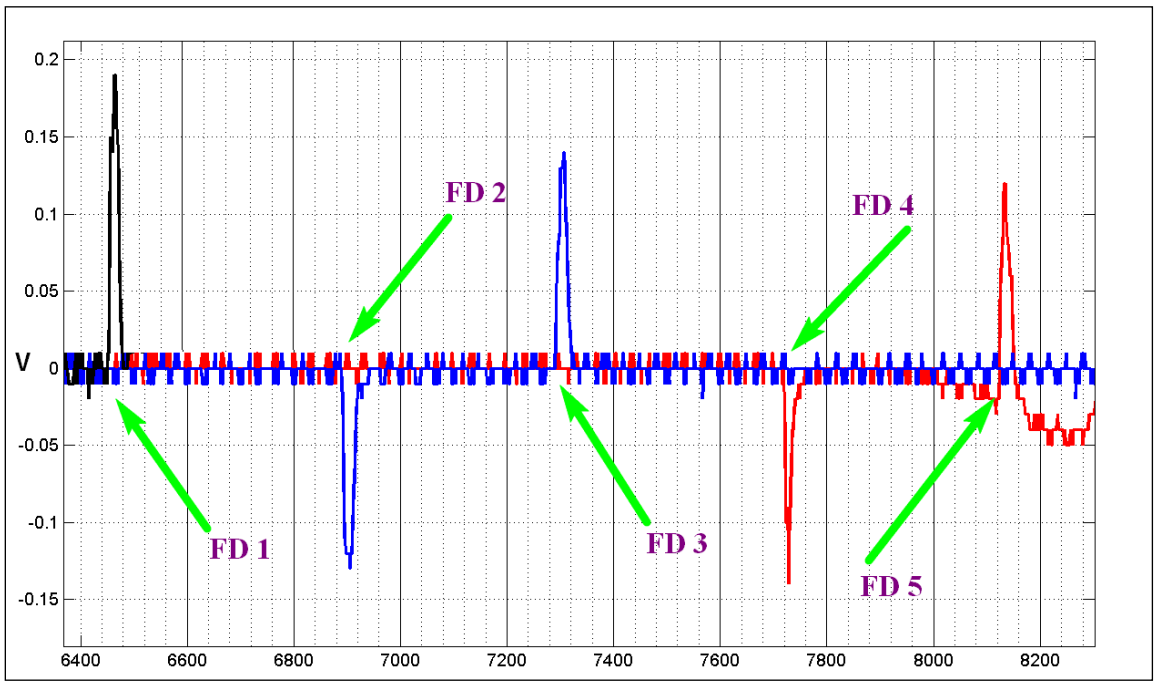

Figure 8. Voltage signal read from the ion sensors from a propagating flame.

Task 1.2 Design and experimental setup of the two Large-scale testing apparatus

Task 1.2.1 Overview of High pressure Steel Flame Reactor Design

A high pressure steel reactor (30.5 cm diameter and 1.2 m in length) with a weight of 0.25 tons was utilized to study flame propagation at the large scale, image shown below in Figure 9. A similar experimental setup used for the smaller reactors was used for this larger steel reactor. This high pressure steel reactor is design to handle pressures of 2.0 – 3.0 MPa.

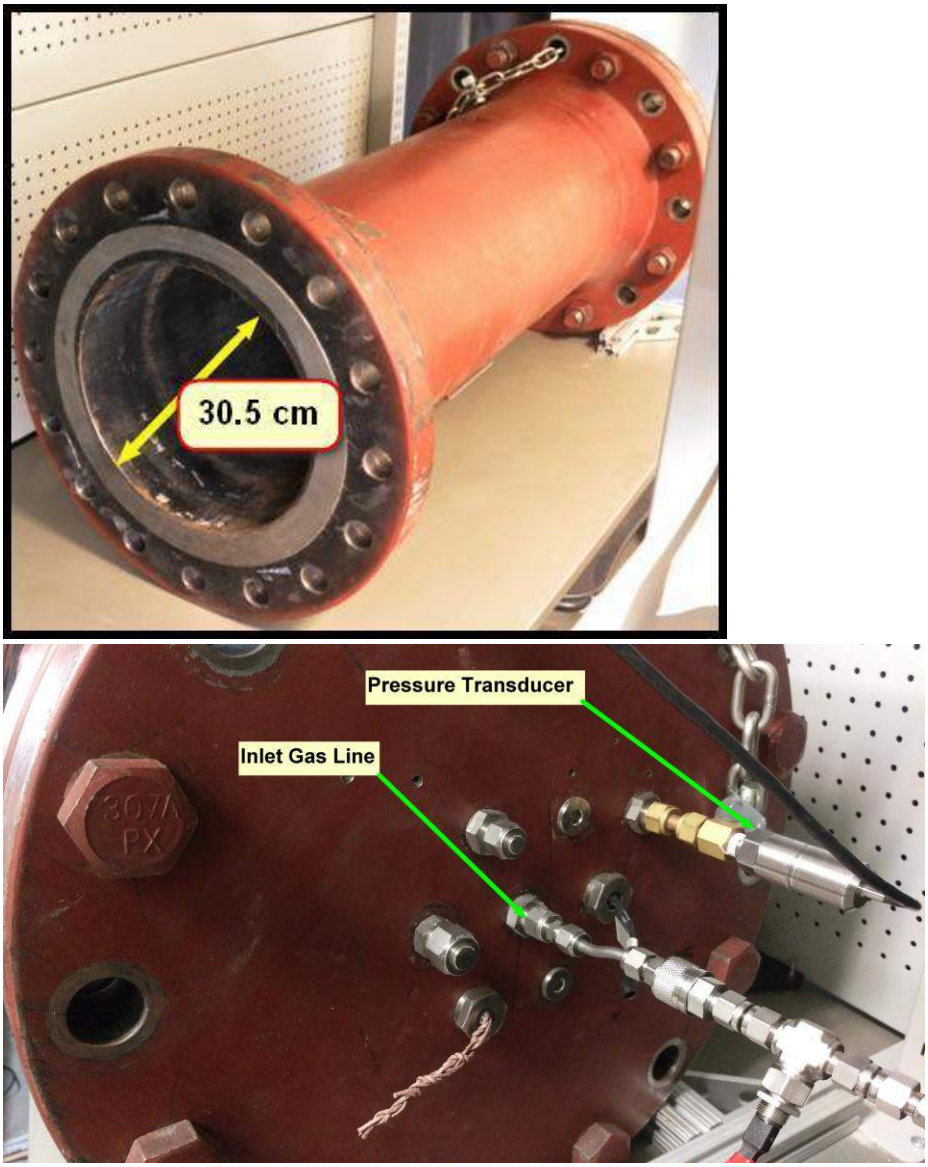

Figure 9. Large steel high pressure flame reactor. Views of open-end and closed-end with multiple ports for gas delivery and sensing (e.g. pressure, temperature, etc.)

Task 1.2.2 Overview of the Explosion Pressure Steel Flame Reactor Design

The largest of the reactors was designed in-house and then contracted using an outside vendor for fabrication. The largest reactor is 71 cm in diameter and 6.1 m long, due to the size and volume of explosive methane-air mixture it was placed outdoors at CSM's experimental Mine Facility. This high pressure steel reactor was design to handle detonations (although this is outside the scope of the present research focus), it is fabricated out of 2.54 cm thick steel with 0.5 ton steel flanges and blind. Additional specifications related to sensor ports and other key dimensions are presented below in Figures 10a – 10c.

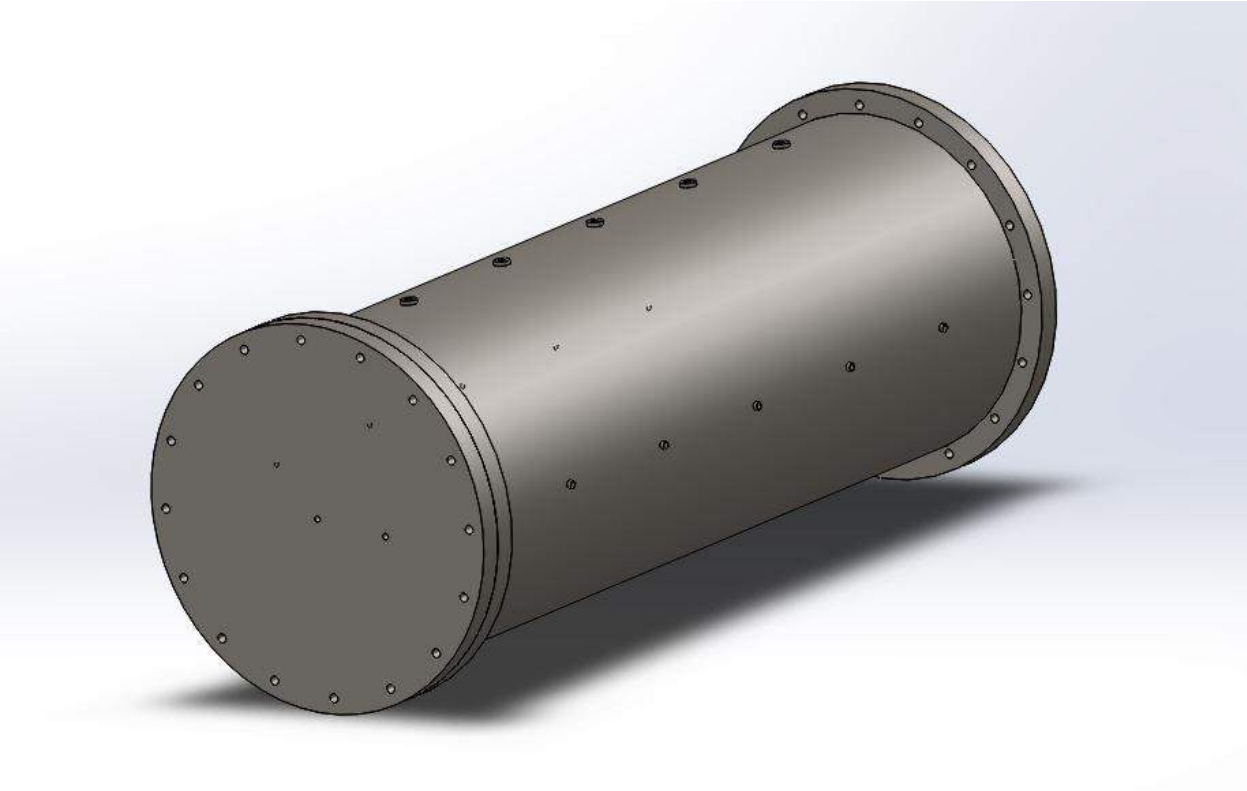

Figure 10a. Three-dimension CAD conceptual drawing of the explosion pressure steel reactor .

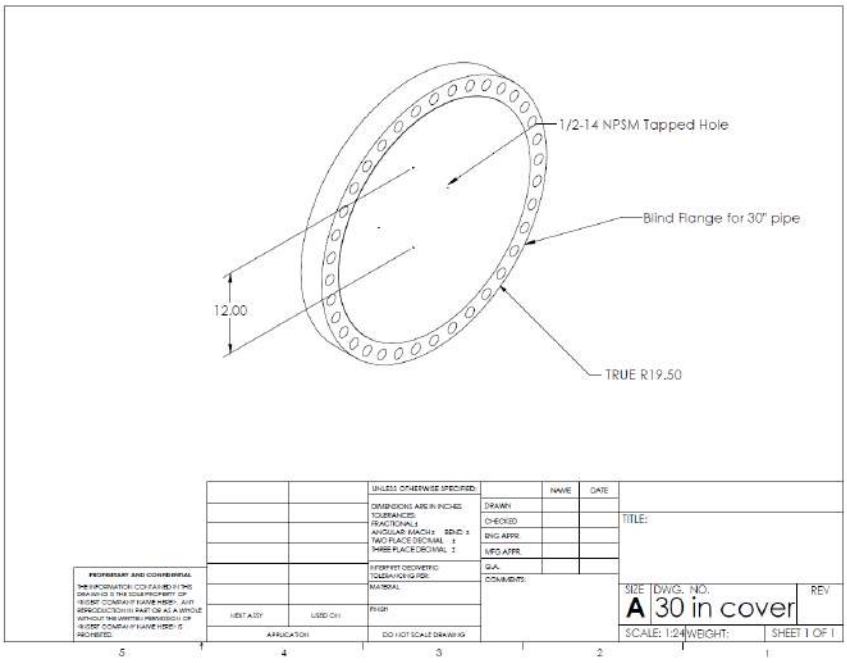

Figure 10b. Two-dimensional CAD drawing of the blind flange drilled and tapped for pipe connections for fuel-air delivery and sensor attachments.

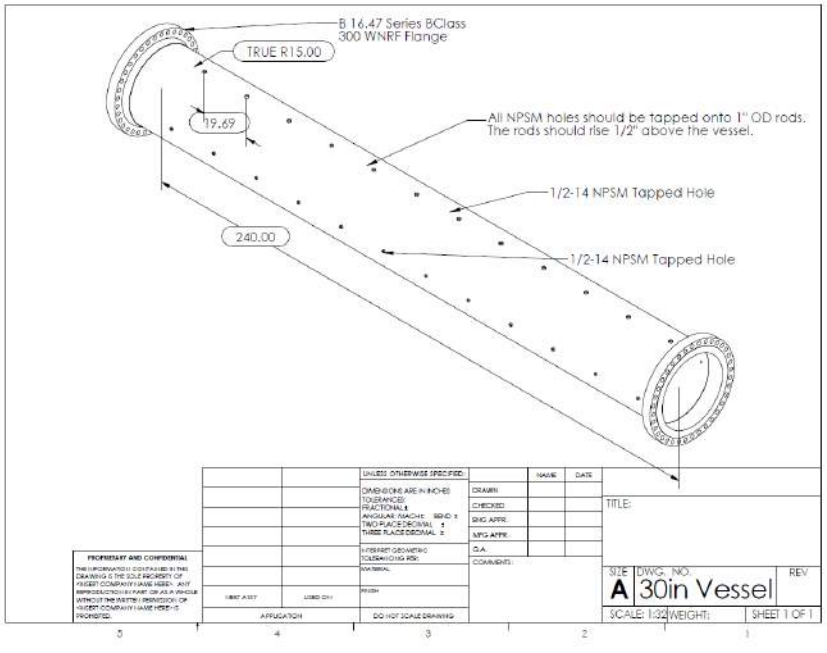

Figure 10c. Two-dimensional CAD drawing of the explosion pressure flame reactor

Task 1.2.3 Experimental Setup for the Explosion Flame Reactor

The experimental setup for this high pressure reactor required some modifications due to being outdoors and the significantly larger volume of explosive gas mixture as it relates to controls, data acquisition and safety. This system consists of four subsystems, which are the high pressure flame reactor, fuel and air delivery system, electrical control and data acquisition system, and the operation control structure. Specifics of the high pressure steel flame reactor are compiled in the Table 1.

Table 1 Specifications of the Explosion Flame Reactor

Property	Value
Weight	4540 kg
Length	6.1 m
Wall Thickness	2.54 cm
Inner Diameter	71.1 cm
Volume	2435 L
Material	Steel
Pressure Rating	>5 MPa
Sensor Ports	24
Rupture Safety Factor	7

It is inside this subsystem where combustion of the fuel-air mixture occurs. As one end of the tube is open to the atmosphere during normal operation, there is no large pressure build up inside the tube beyond a slight rise due to the expansion of exhaust gasses. This open-ended design is the primary engineering safety control against undesired pressure rises inside the reactor during combustion. Based on extensive laboratory testing, this is more than adequate to control pressure within the deflagration regime.

The fuel and air delivery system consists of the standard 17 MPa fuel and air supply cylinders, a cabinet which houses some of the valves and controllers, a supply line and a mixing tank, and various valves and fittings connecting high pressure Swagelok tubing. The major components of this system are illustrated below in Figure 11. Note that the cabinet is not shown, for clarity. There are 3 gas cylinders, located approximately 12 feet behind the closed end of the flame tube. These consist of the fuel, air and inert purge gases. These cylinders have gas lines leading from them to the cabinet which houses the mass flow controllers (MFCs) and two electrically operated solenoid valves shown in Figure 12. There are two gas lines leading from the cabinet to the mixing tank, one consisting of air and the other of either fuel or purge gas, these lines are buried in a shallow trench and rest inside a section of PVC piping for protection, the mixer is within 12 inches of the heavy flange that makes up the closed end of the flame tube as shown in Figure 13.

For this reactor (Figure 14), an alternative sparking method is needed for remote control. To this end a circuit was designed and tested which uses a 12-Volt battery and an automotive ignition system hooked to a self-shorting relay, circuit diagram shown below in Figure 15. The spark produced by the sparking circuit is not continuous, but rather pulses at the frequency of the switch inside the relay. This system was tested on the other flame reactors and found to be

effective and produce no noticeable difference in flame velocities from those produced by the single piezo-electric ignition system. An image of the spark produced by this system is shown below in Figure 16.

The electrical control and data acquisition system consists of a laptop PC with MATLAB control software installed, NI-DAQ cards, and the wires that carry the low-voltage signals back and forth. The software controls the 3-way valve, the 2-way valve and the mass flow controllers, all of which are located inside the cabinet. The software also controls the 3-way purge valve and collects data during and experiment via connections mounted inside the sensor ports along the body of the flame tube. Flame detectors were placed along the length of the reactor to detect the propagating flame as shown in Figure 17. Heavy duty foil is lightly secured to the open end of the vessel to contain the explosive methane-air mixture prior to ignition as shown in Figure 18.

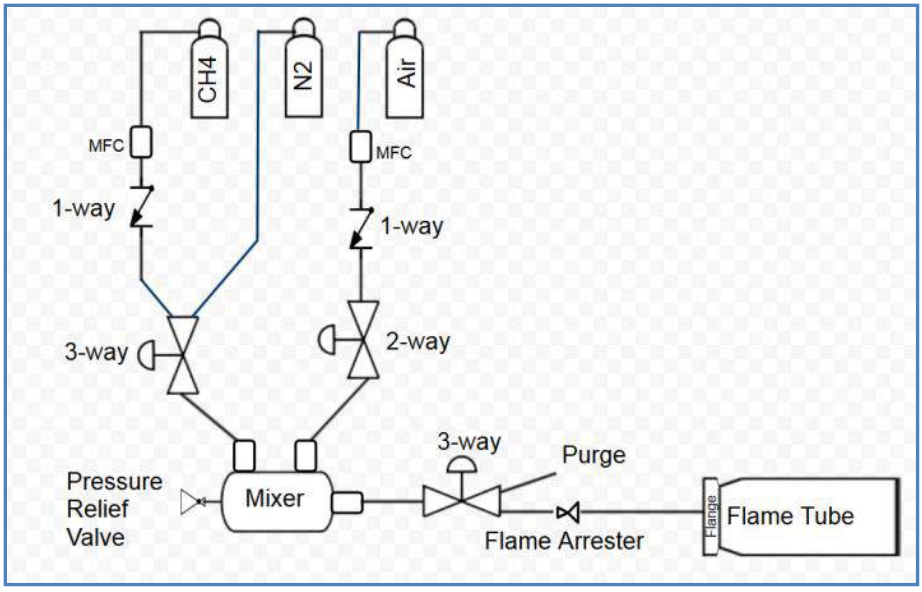

Figure 11. Process flow schematic for the explosion flame reactor.

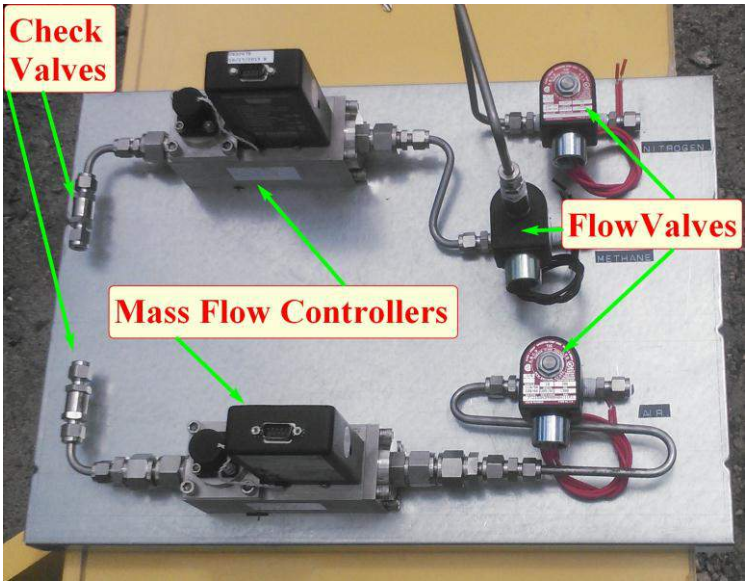

Figure 12. Layout within the flow control cabinet.

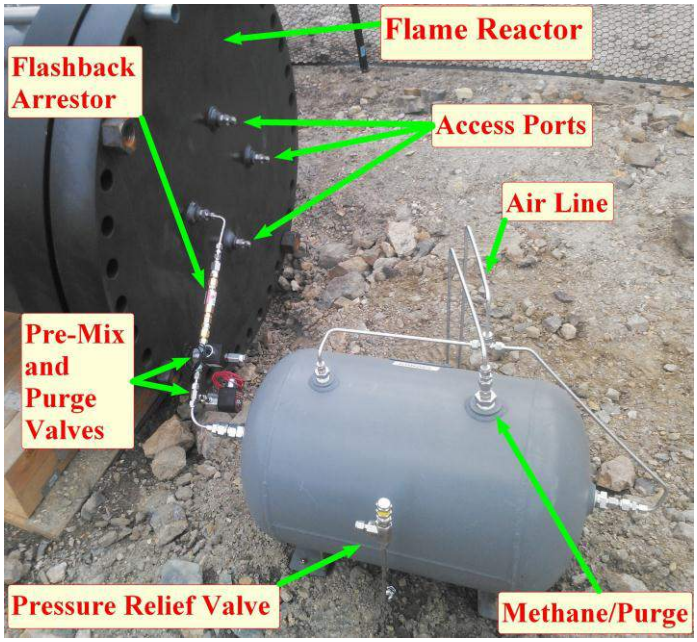

Figure 13. Plumbing for fuel, air, and inert gas and mixing tank near closed end of flame reactor.

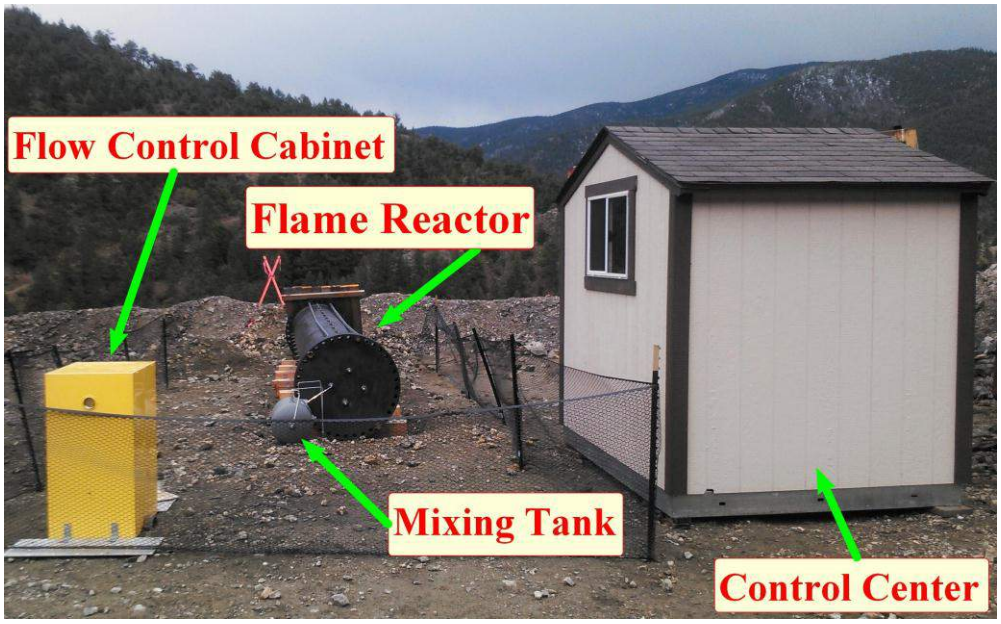

Figure 14. The control cabinet, mixing tank, and explosion flame reactor.

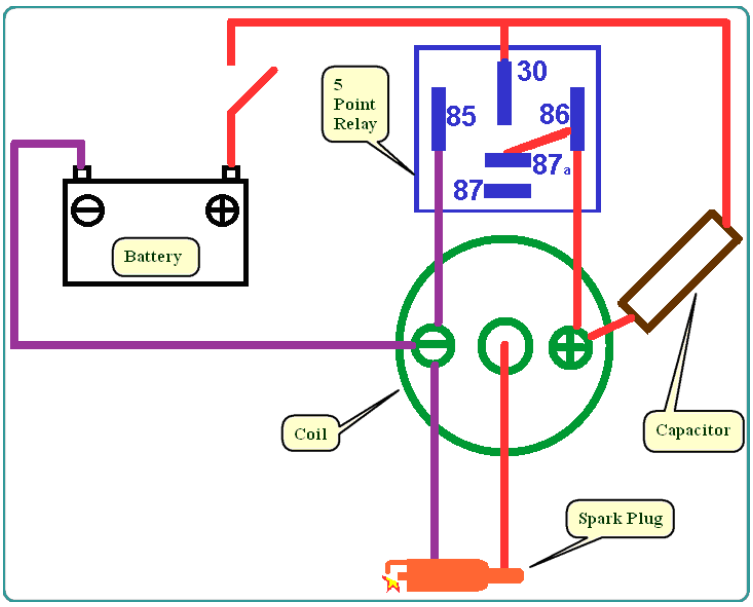

Figure 15. Ignition circuit diagram used for remote ignition

Figure 16. Spark produced by the remote ignition system.

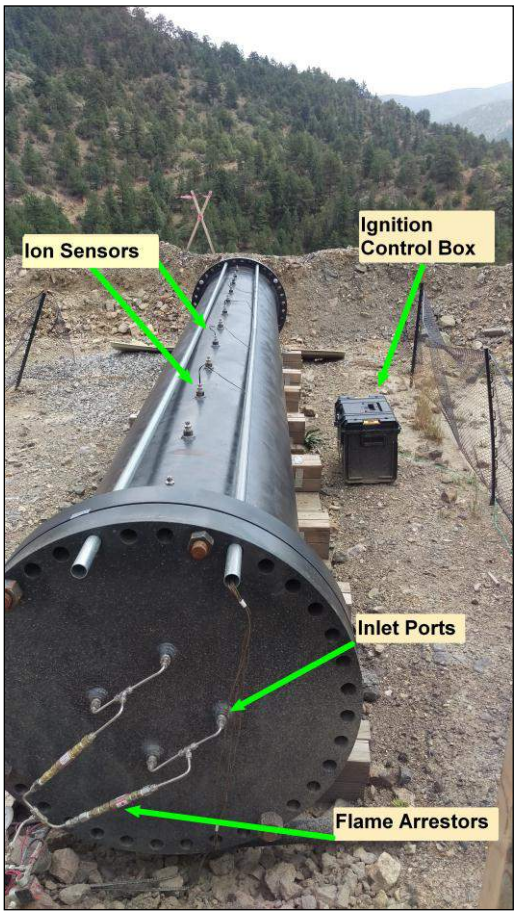

Figure 17. Explosion flame reactor showing ion sensors and remote ignition control box.

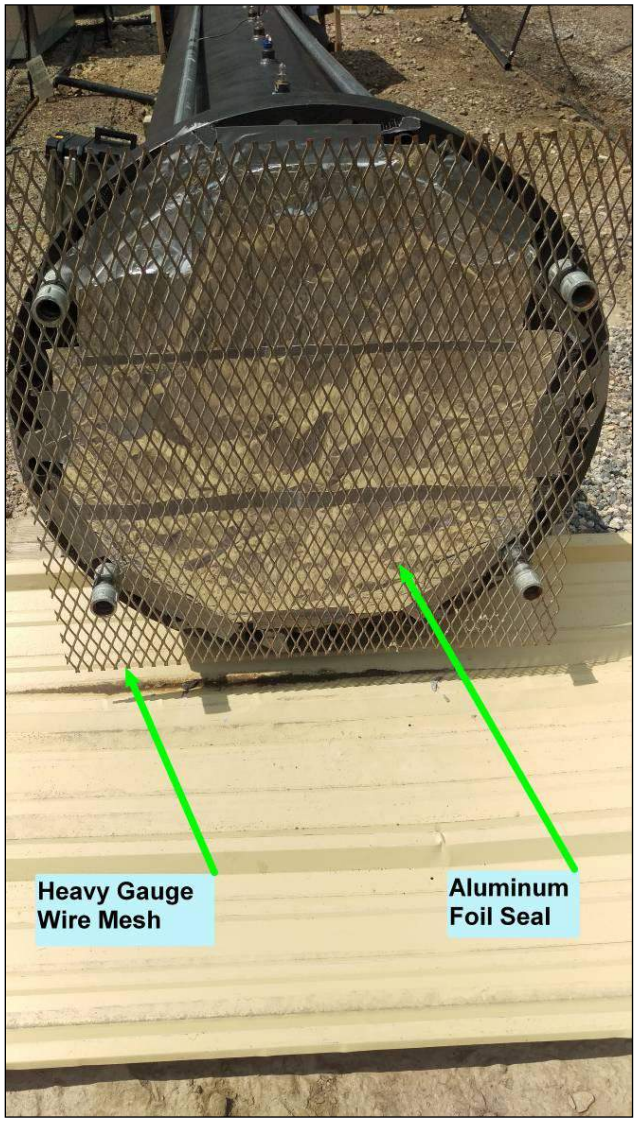

Figure 18. End view, showing end safety screen and foil seal. The foil was used to contain the explosive methane-air mixture prior to ignition. The heavy gauge screen prevents debris from exiting the flame reactor and containment of the heavy duty foil after explosion test.

Task 1.3 Experimental test parameters

The three largest reactors listed above were used to measure methane flame propagation velocities with and without simulated Gob inserts. The experiments without the simulated Gob insert provides a reference point for methane ignition and propagation. Tests were conducted with ignition at both the open-end (slowest burning velocity) and closed-end (fastest burning velocity) to bound the range of burning velocities expected with the simulated Gob. The simulated Gob inserts consisted of rocks of various sizes and material properties placed inside the reactor vessels and confined with steel mesh hardware cloth. The hardware cloth was chosen with spacing much larger than the quenching distance and with thin gauge wire to minimize the heat losses and fluid dynamic interactions with the propagating flame. Details of the various parameters (e.g. permeability, rock size, porosity of the rock, moisture content, temperature, etc.) investigated with the simulated Gob with respect to each flame reactor are listed below.

Several simulated Gob conditions were investigated to cover a wide range of possible conditions which could be present within the Gob area. The wide range of conditions also provides an extensive experimental database for validation of a robust model.

Rock rubble permeability and barrier length

Rock rubble permeability and barrier length was varied to capture the variability of rock rubble in the Gob area and to simulate varying locations of the EGZ and distance inby the longwall face by varying the barrier length. The barrier length was varied between the various reactors to maintain a constant percentage (tests were performed for 3.3% and 6.6%) of the reactor length filled with rock rubble across the various scales of the reactors.

Variation in rock material used in simulated Gob

Three different rock materials were used to provide insight into the impact different Gob material could have on methane explosions. The goal is to recreate the variability in Longwall Gob rock rubble due to different overburdens based on the location of the mine.

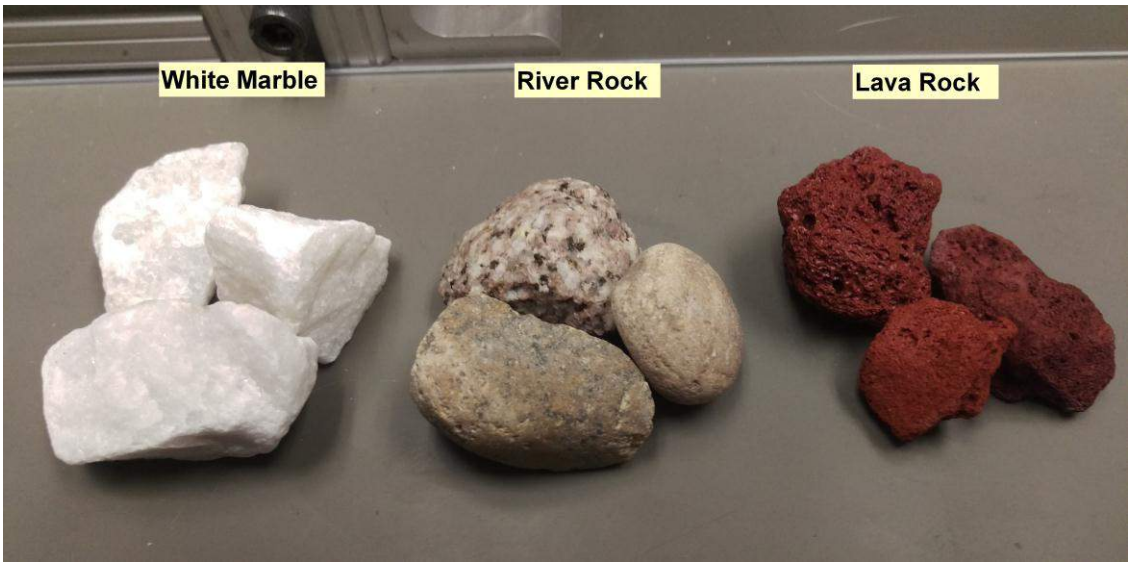

Figure 19. Various rock materials used to simulate different roughness, porosity and thermal conductivity.

Table 2: Rock material properties

Material properties	White Marble	River Rock (Granite)	Lava Rock (Basalt)
Thermal conductivity (W/m-k)	2.5	2.3	1.7
Porosity	<1%	<1%	35%
Density	2.6 g/cm^3	2.8 g/cm^3	3 g/cm^3 (matrix)

Varying the moisture content of the rock rubble.
Moisture levels (i.e. humidity) was investigated to simulate different environments which may be present in the gob either from the moisture contents of the overburden when the roof collapses or the ambient air may contain various levels of saturated water which will impact the ambient humidity. For these studies the relative humidity was varied from 10% to 16%.

Varying the explosive methane-air mixture concentration.
A range of explosive homogeneous methane-air mixtures (methane vol. %, 8.2, 9.5, 10.8) within the explosive limits were investigated to determine the impact on burning velocity and risk of transitioning from a deflagration to detonation wave. The methane-air mixtures were chosen in the explosive range typically found in Coward's triangle (see Figure 20.), which is a commonly used in the mining industry.

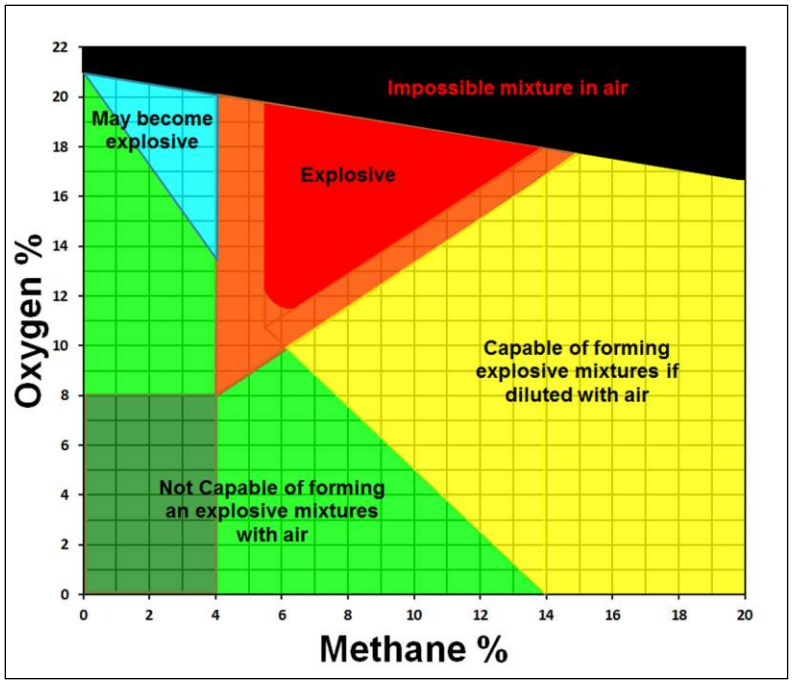

Figure 20. Methane-air mixture diagram color coded Coward's triangle.

Task 1.3.1 13.6 cm quartz flame reactor

Tests were performed with the13.6 cm quartz reactor to investigate the effects of varying rock and ambient parameters. These experiments were performed at 22 °C and at a local atmospheric pressure of 81 kPa. Three different kinds of rocks were used for these tests. Two of the rocks, the granite and marble, are non-porous, while the basaltic lava rock is highly porous. The moisture content was varied by spraying water on the rocks and allowing for evaporation as the filling air flowed through the rocks. This resulted in a variation in relative humidity from 10% to 16%. As elsewhere, the methane concentration was varied between lean and rich cases. The rock barrier length was also varied from 3.3% to 6.6% of the reactor vessel length. The variability of burning velocity as a function of rock sizes for fixed plug length was also tested with this reactor.

Table 3. Simulated Gob conditions for the 13.6 quartz flame reactor

Rock rubble barrier length (cm)	Rock rubble barrier height (cm)	Rock rubble sizes (cm)	Rock material	Moisture content of the rock rubble (% RH)	Explosive methane concentration (%)
5.1	10.2	2.9, 4, 9	Granite, Basalt, Marble	10, 16	8.2, 9.5, 10.8
10.2	10.2	2.9	Granite	10, 16	8.2, 9.5, 10.8

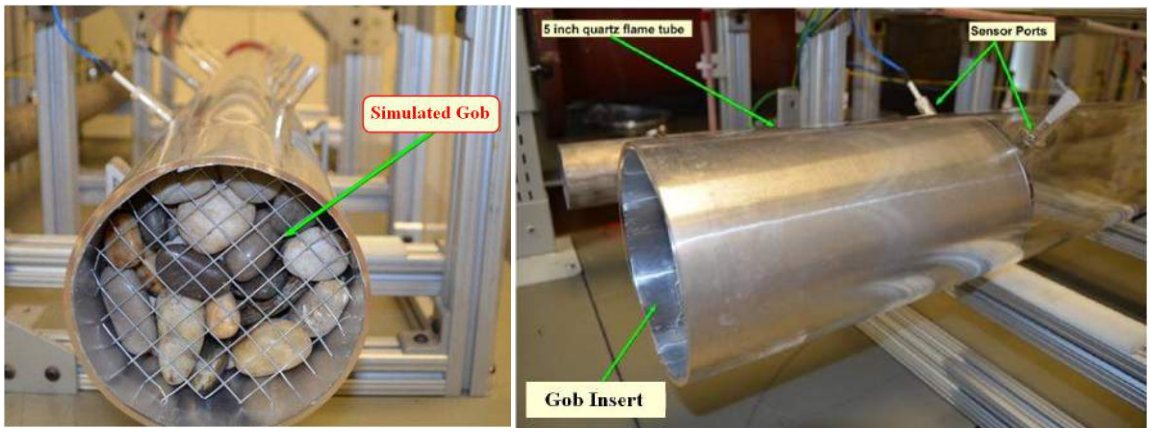

Figure 21. Rock rubble insert with metal cylinder for simulated gob experiments in Quartz reactor.

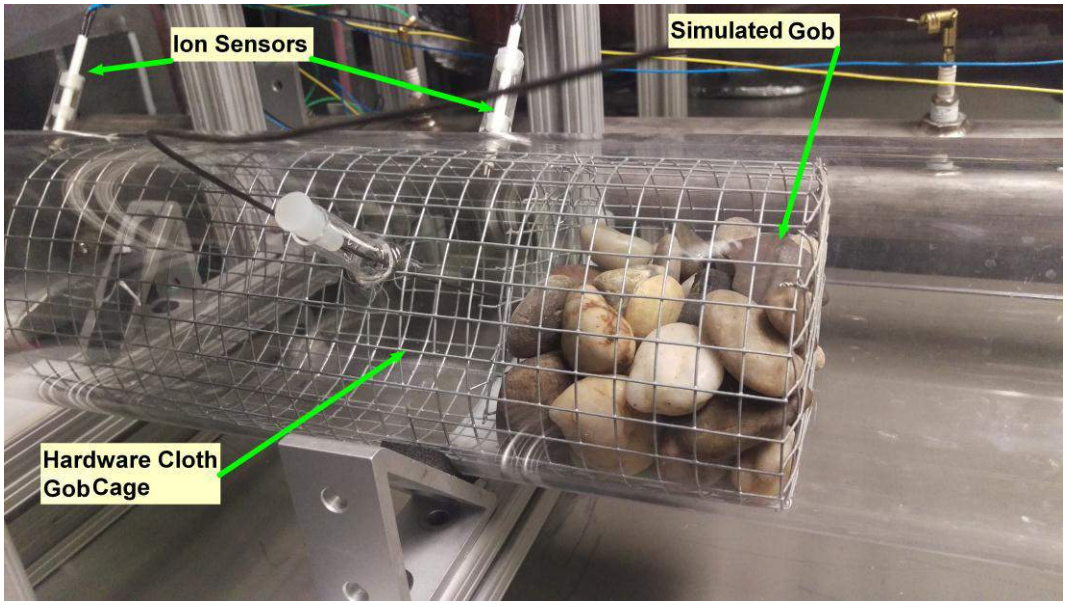

Figure 22. Rock rubble insert using hardware cloth. Allows visualization of flame as it propagates through the simulated Gob.

Task 1.3.2 30.5 cm high pressure flame reactor

Tests were performed with 30.5 cm steel reactor to investigate the effects of varying rock and ambient parameters. These experiments were performed at 22 °C and at a local atmospheric pressure of 81 kPa. Two different kinds of rocks were used for these tests. The moisture content was varied by spraying water on the rocks and allowing for evaporation as the filling air flowed through the rocks. This resulted in a variation in relative humidity from 10% to 16%. As elsewhere, the methane concentration was varied between lean and rich cases. The rock barrier length was also varied from 3.3% to 6.6% of the reactor vessel length.

Table 4. Simulated Gob conditions for the 30.5 steel flame reactor

Rock rubble barrier length (cm)	Rock rubble barrier height (cm)	Rock material	Moisture content of the rock rubble (% RH)	Explosive methane concentration (%)
4.1	22.8	6.35	10, 16	8.2, 9.5, 10.8
8.2	22.8	6.35	10, 16	8.2, 9.5, 10.8

Figure 22. Rock rubble insert for simulated gob experiments in high pressure reactor (30.5 cm)

Task 1.3.3 71 cm explosion flame reactor

Tests were performed with the 71 cm steel reactor to investigate the effects of varying rock and ambient parameters. These experiments were performed at 22 °C and at a local atmospheric pressure of 81 kPa. As elsewhere, the methane concentration was varied between lean and rich cases. The rock barrier length was also varied from 3.3% to 6.6% of the reactor vessel length.

Table 5. Simulated Gob conditions for the 71cm steel flame reactor

Rock rubble barrier length (cm)	Rock rubble barrier height (cm)	Rock rubble sizes (cm)	Rock material	Explosive methane concentration (%)
20.2, 40.4	53.3	15.2	Granite	8.2, 9.5, 10.8

Figure 23. Rock rubble insert for simulated gob experiments in explosion flame reactor (71 cm)

Barriers with Task 1

It should also be noted that the fabrication of the largest of the flame reactors was delayed due to several unexpected events (change of vendor, approval of budget adjustments, and weather, details provided in the two quarterly reports) outside the control of the researchers, these unforeseen events along with the normal time for safety approval from the University's Environmental Health & Safety (EH&S) department resulted in the largest reactor (71 cm diameter and 6.1 m long) not coming online until towards the latter months of the project (**July 2015**). With that being said, the second of the largest (30.5 cm diameter and 1.2 m long) reactor provided sufficient experimental data in conjunction with the 71 cm reactor across the various gob parameters to allow sufficient validation of the combustion model. Details of the experiments ran in each flame reactor are provided in section 4.0.

Task 2 - Development and Validation of Combustion model

Concurrently with the experimental effort, a modeling effort was undertaken with the ultimate goal of arriving at a full-scale model of the combustion of an explosive gas zone in a longwall mine. This process was initiated by studying the dynamic flame behavior using a simplified 2-D planar channel models corresponding to the above experimental reactors. These simplified models allowed for quick turn-around during the verification and validation process, they also allowed for the development and validation of computational techniques such as grid adaption and adaptive time-stepping for accurately tracking the thin chemical reaction zone (i.e. flame). These models also provided insight into how methane flames transitions through the simulated gob.

A commercial package (ANSYS 15.0 Fluent) was used for all combustion modeling because of its wide availability, and to allow models developed within to be used by anyone else in the industry for the development of mitigation strategies. For all models, the species transport, energy equation, and laminar settings were used. Stoichiometric parameters followed the range discussed above. Global, 1-step kinetics (see Rxn. 1 and Eqn. 1) were used to model the reaction of methane with air. Ideal gas behavior was assumed for the density, and heat capacity and viscosity values of air as a function of temperature were used from NASA data tables. Model operating temperatures and pressures were chosen so as to simulate laboratory ambient conditions of 300 K and 100 kPa.

The overall chemical reaction under consideration is the combustion of methane in air, given by the following global reaction and reaction rate

$$CH_4 + 2\left(O_2 + 3.76N_2\right) \rightarrow CO_2 + 2H_2O + 7.52N_2 \qquad \text{Rxn. 1}$$

$$\frac{d\,[CH_4]}{dt} = A_k T^{\beta_k} \exp\left(-{}^{E_k}/_{RT}\right)[CH_4]^m[O_2]^n \qquad \text{Eqn. 1}$$

The entries correspond to the parameters used with the Arrhenius rate equation, shown above. In this equation, A_k is the pre-exponential factor, β_k is known as the temperature exponent, E_k is the activation energy, and the letters *m* and *n* are the species concentration rate exponents. These parameters together give the rate of conversion of the fuel to the combustion products.
The units of the differential are kmols/(m^3-sec), the units of E_k (J/kgmol), and the units of A_k are consistent with the concentrations expressed in kmol/m^3.

Table 6 Mechanism parameters for use with the Arrhenius equation.

Mechanism	A_k (kmol/m^3)	β_k	E_k [J/kgmol]	m	n
ANSYS Default	2.19e+11	0	2.027e+8	0.2	1.3

ANSYS 15.0 2-D planar model Settings

The following settings were used in ANSYS Fluent throughout the solving process.

- 2-D planer fluid settings.
- Global one-step reaction
- SIMPLE velocity coupling solver
- STIFF chemistry solver for integration of kinetics
- 2nd order implicit solver for time integration
- Adaptive time-stepping with minimum dt = 1 x 10^{-6} sec and maximum dt = 2 x 10^{-5} sec
- Ideal Gas behavior for gas density changes
- Kinetic theory for gas mass diffusivity
- Linearly interpolated values for thermal conductivity and viscosity as a function of temperature
- Laminar flow
- Planer symmetric stagnant flow
- Walls radiating to 300 K
- Initial mesh size of 0.5 mm
- Adaptive meshing set to adapt on the gradient of the kinetic reaction rate, with a maximum refinement level of 2, every 5 time steps
- All convergence monitors set to 1x 10^{-6}, except species, which were set to 1 x 10^{-4}

Initial setup for ignition of methane

The second task was to model the flame propagation velocity observed and measured experimentally in the reactors. The model was originally built using the ANSYS spark model in version 14.5. This model proved to be unsuitable for modeling a traveling flame in stagnant gas. In the release notes [21] for version 15.0, the previous spark model was acknowledged to be "extremely sensitive to grid size, time-step and spark parameters," as these investigators discovered. Even the newer spark model, though it is said to slowly ramp up combustion within the spark radius, produces too rapid an expansion in stagnant gas and gives rise to a high velocity pressure wave more akin to a detonation than a deflagration. This pressure wave seems to initiate what looks like a flame that quickly dissipates as the wave passes, as seen in Figure 24. In the top image of Figure 24 a thin line of high kinetic activity can be seen a small distance away from the circular spark. This is the flame propagating away from the spark as it should. In the bottom image, the pressure wave which initiated this reaction zone is seen. The pressures are much higher than seen experimentally, and this wave moves much faster than any deflagration wave measured for this project. As the high-speed wave moves past about 2 spark diameters, the flame invariably extinguishes behind it. More work is needed to tune the spark model to accurately capture the deflagration wave.

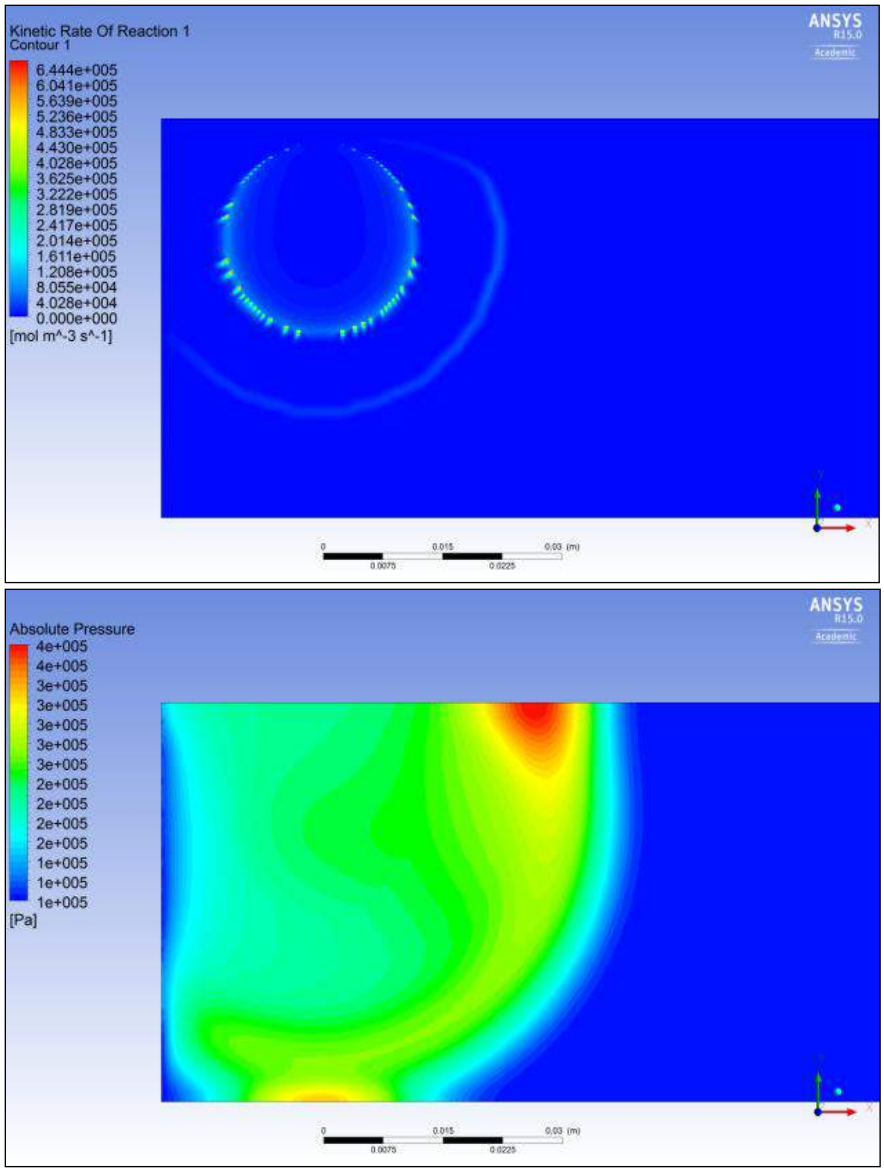

Figure 24. The failure of the ANSYS spark model to produce a propagating flame in stagnant gas. The initial temperature and pressure is 300 K and 101 kPa. Spark energy is 8 mJ and duration is 1 ms.

Based upon the apparent problems found in the ANSYS spark model, an alternative ignition model was chosen for the remainder of the modeling. The new ignition source is the model of a hot ignition plate. In Fluent this is modeled as a small (~ 1 mm square) wall with a constant temperature high enough to initiate combustion in the adjacent gas molecules. A wall temperature of 2300K was chosen, this agrees with the approximate temperature of the burned gas, and thus was a good starting place. This approach produced a deflagration whose flame speeds were similar to those measured experimentally. Figure 25 shows the development of the flame of the initial flame kernel; further details of the results will be presented in section 5.0.

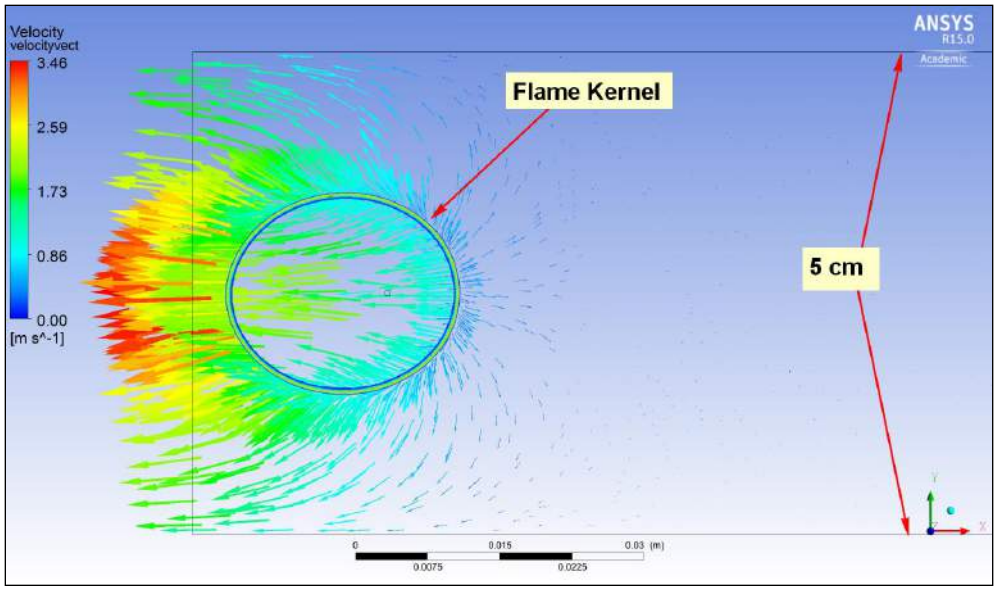

Figure 25. Initial Spark kernel, showing exhaust of gasses from the open end of the tube. The thick ring is the flame front. Stoichiometric methane-air (methane is 9.5% by vol.) mixture, at 300 K and 101 kPa.

Task 3 - CFD model of longwall gob and impact of EGZs:

The goal of this task was to develop an integrated mine-scale model capable of predicting EGZs and simulating methane-air explosions to determine the specific hazards that miners may face as a consequence of such explosions. The other goal of this integrated mine model was to provide guidance for attaining safe conditions (distance from face, volume and gas composition) that must be maintained to control the safety hazard from EGZ explosions.

The insights gained from the previous two tasks were used to integrate the combustion model into a three-dimension model of a longwall coal mine ventilation system which was capable of predicting EGZs. The specific ventilation design modeled is a progressively sealed Gob using a ventilation pattern with nitrogen injection on the headgate and tailgate sides of the panel as seen in Figure 26. Gob Ventilation Boreholes (GVBs) are operating to extract mine gas before it enters the ventilation system at a rate of 0.17 m^3/s (350 cfm) each. Fresh air is supplied to the face at a rate of 33 m^3/s (70,000 cfm), and nitrogen is injected at a rate of 0.19 m^3/s (400 cfm) on both the headgate and tailgate sides.

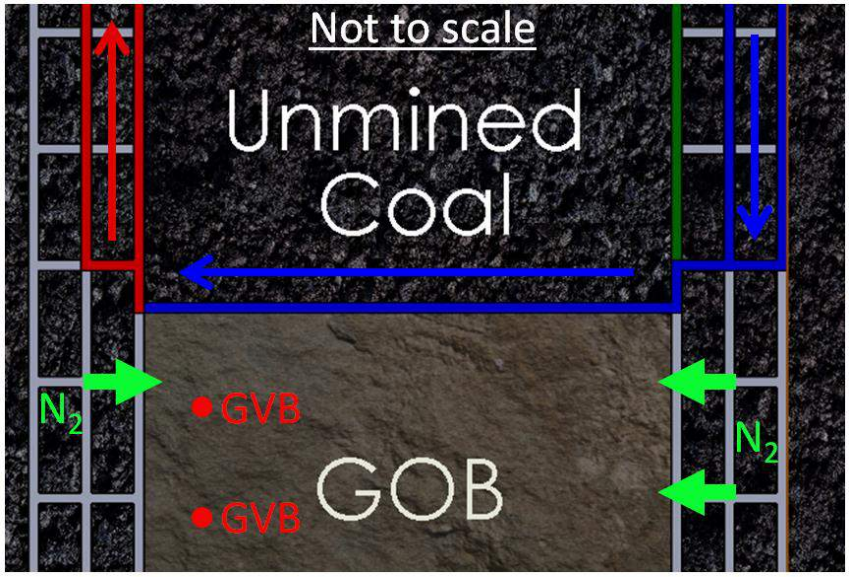

Figure 26. **Progressively sealed U-type ventilation plan view layout.**

In order to model the combustion chemistry of a methane-air mixture, proper scaling of large mine ventilation models was required, which has approximately 9 million cells. Figure 27 shows a detailed view of the mesh of the shields.

The presence of methane-air in explosive mixtures was identified by Marts et al., 2014 [22] progressively sealed gob ventilation systems when using a U-type pattern in CFD simulations by researchers at CSM; an example of small EGZ located directly behind the shields near the tailgate and in the tailgate is shown in Figure 28.

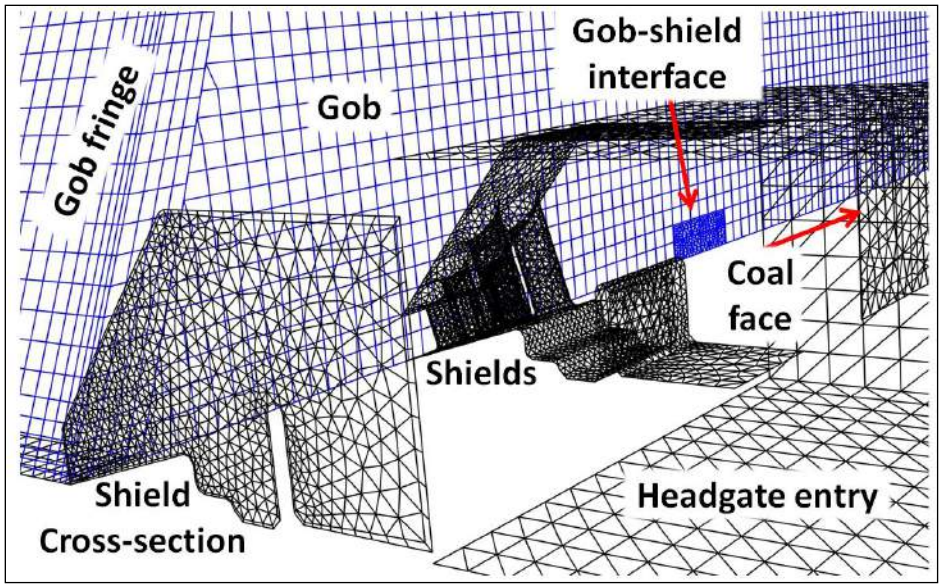

Figure 27. 3D Mesh of the longwall face and Gob immediately behind the shields.

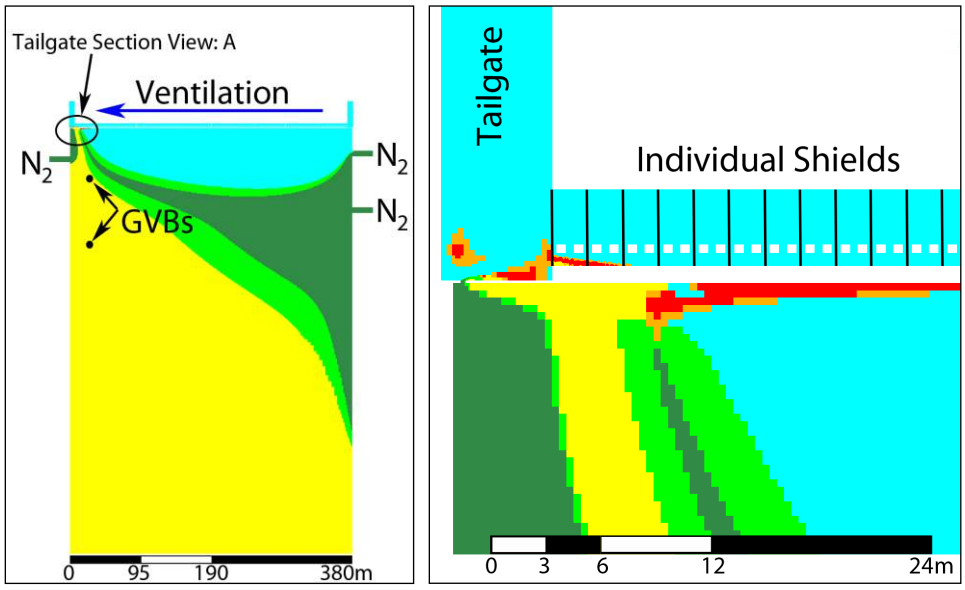

Figure 28. Explosive gas zone (EGZ) plot of a progressively sealed gob using U-type Ventilation. Tailgate Section View A is enhanced on the right side to show EGZ (red color)

The flow conditions at the boundaries are exported as profiles and a constant inlet velocity, pressure inlet, or pressure outlet with the associated species concentration is used. The model is then solved to convergence in a steady-state simulation to resolve any geometry mismatches between the large ventilation model, which used only hexahedron cells and right angles, and the more detail tetrahedron mesh of the shields. Results of the coupling of the combustion model into the three-dimension CFD model of the longwall mine is presented below in section 5.0.

5.0. Summary of Accomplishments and Innovation Highlights

Summary of accomplishments

The focus of this short-term exploratory research project was three-fold. First was building an experimental facility capable of studying methane flames in the presence of rock rubble to provide insight into how a methane explosion would behave in the gob area of a longwall coal mine. Second, was to utilize the data from the experiments conducted as part of the first task to develop and validate a combustion model for methane flame propagation through rock rubble. Lastly, taking the combustion model and incorporating this model into a three-dimensional CFD model of a longwall coal mine and developing a model which could not only predict the location and size of EGZs, but could also predict the impact of an explosion if it were to occur. The ultimate goal of the proposed research wa**s the development of a CFD model of the longwall gob which can simulate EGZs based on various ventilation schemes and includes a combustion model to simulate explosions within the gob to determine the explosion hazard to miners**. Each of the three tasks proposed were accomplished with the development of a preliminary model capable of predicting the a methane explosion and the transition to detonation with an extreme rise in pressure. Details of the results and accomplishments for each task are presented below.

The results of this exploratory research project provides sufficient evidence for moving forward with a more extensive investigation of the dynamic interactions of the flame and rock rubble, leading to a more refined model via a multi-year project with the end result being a fully-developed model for use by mining engineers to assist in mitigation strategies for potential explosions hazards.

Detailed summary of results and accomplishments with each Task

Task 1 – Experimental investigation of methane flame propagation through simulated Gob (i.e. rock rubble) with the small-scale and large-scale Gob Explosion Simulation Apparatus

Task 1.1 – Methane flame propagation no simulated Gob

This task was to provide a reference point for how the methane flame behaves in an empty horizontal reactor. This task provided insight into the how the flame transitions from a flame kernel to a turbulent flame using the 13.6 cm quartz reactor and high-speed imaging; this was a crucial step for initial validation of the model in ensuring the physical transition of the flame was being captured. A second objective was to determine the impact of physical scale on methane burning velocities which is important since even the largest reactor is not on the scale of an actual Gob area in a Longwall coal mine. Also having multiple scales is crucial in determining whether the combustion model would accurately predict burning velocities at the mine scale if there was not at least two reference points, hence one of the motivation for the modification from the original proposed research of having one large reactor for testing. The third objective was to capture the effect of location of ignition source on the burning velocity as it was expected the slowest velocities would occur with ignition occurring at the open end and the fastest occurring at the closed end, and the rock rubble producing burn velocities between the two conditions. The open end ignition produces the slowest burning velocities due to the hot product gases being allowed to expand into the atmosphere and the flame compressing the unburned gases upstream of the flame which will increase in pressure pushing back against the flame limiting the burning velocity. Whereas, the closed end ignition will produce the highest burning velocities due to the hot products being forced into a relatively small volume and increasing in pressure which in turns pushes against the flame, this is coupled with the effect that the upstream unburned gases are not increasing in pressure as the flame propagates towards the open end resulting in no opposing forces against the flame.

Task 1.1.1 – Visualization of the methane ignition and transition to turbulent flame

Initial experiments investigated the ignition and transition of methane flame kernel to a turbulent (wrinkled laminar regime) flame, images of this transition can be observed in Figure 29. It is crucial to capture the fundamental behavior as the flame transitions along with propagation velocities as this will become important when the flame dynamics become coupled with the rock rubble as presented in the next section.

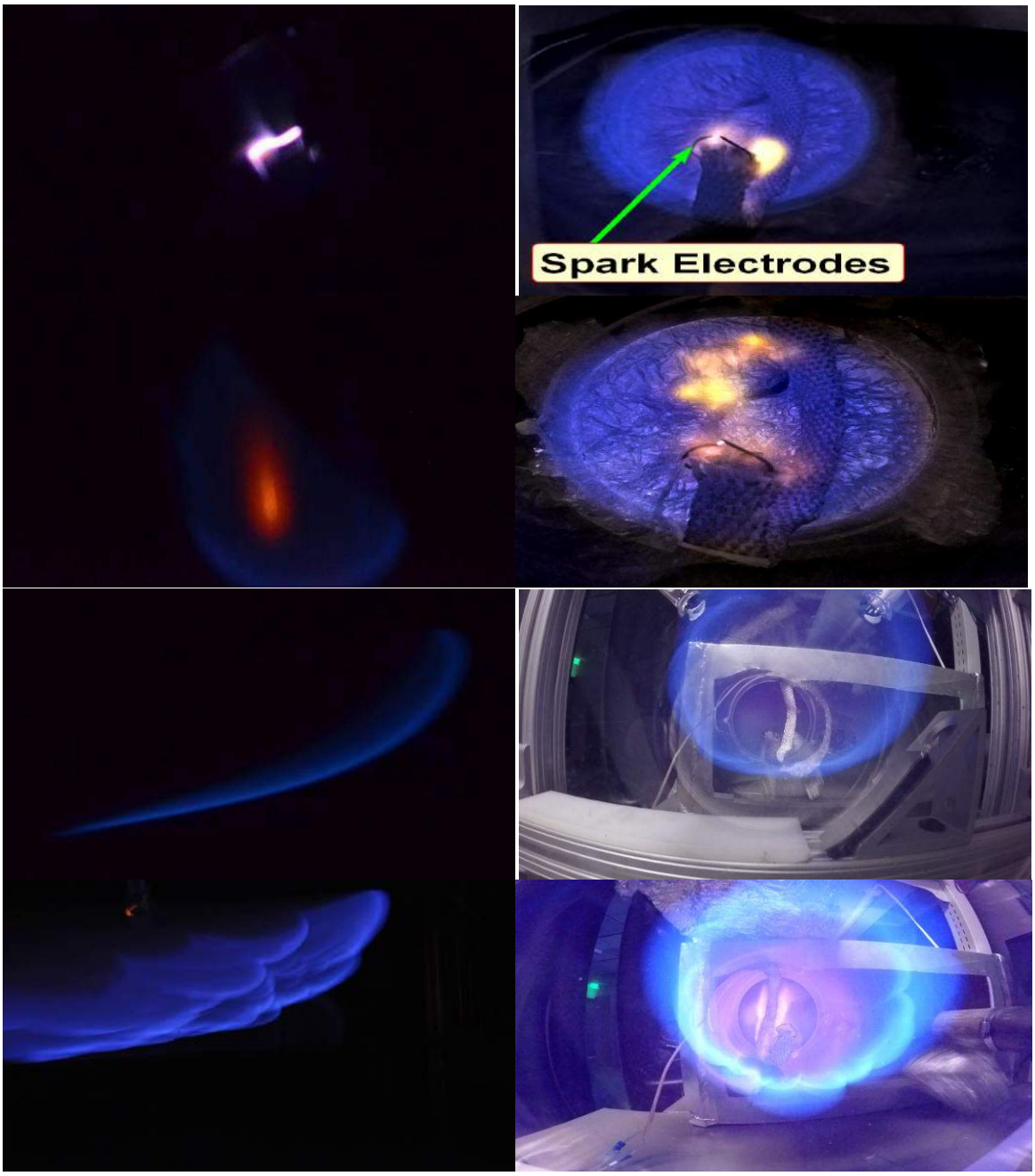

Figure 29. Methane ignition, and transition from spherical flame kernel to turbulent flame (left-images provide side profile view; right-image provide axial view). From top to bottom, we have

the initial spark and flame kernel. Then we see the growth of the flame as it spreads out from the electrodes. The third row shows the laminar propagation of the flame as it begins the journey along the reactor. The fourth row shows the beginning of the wrinkled laminar or transitional stages.

Task 1.1.2 – Methane burning velocities as a function of reactor size and methane-air mixture concentrations

A premixed mixture of methane-air is delivered to the each reactor and is ignited from the open end of the tube. Maximum burning velocities were seen at stoichiometric conditions and fall-off at both lean and rich conditions as expected from theory, shown below in Figure 30.

Propagation velocity increases for all fuel-air ratios with size of reactor. In all cases, the velocity in the reactor was taken to be the velocity between sensors where the flame was most uniform, before the onset of wrinkling, when possible. Otherwise, the speed between the second and third sensor (details of sensor spacing listed for each reactor in section 4.0) was used based on observations with the quartz reactor. This allows enough space for the uniform propagation to materialize, but is not long enough for turbulence to form and dominate. Even with this consideration, the measured velocities did not vary more than 12% on average from sensor to sensor along the length of the reactor.

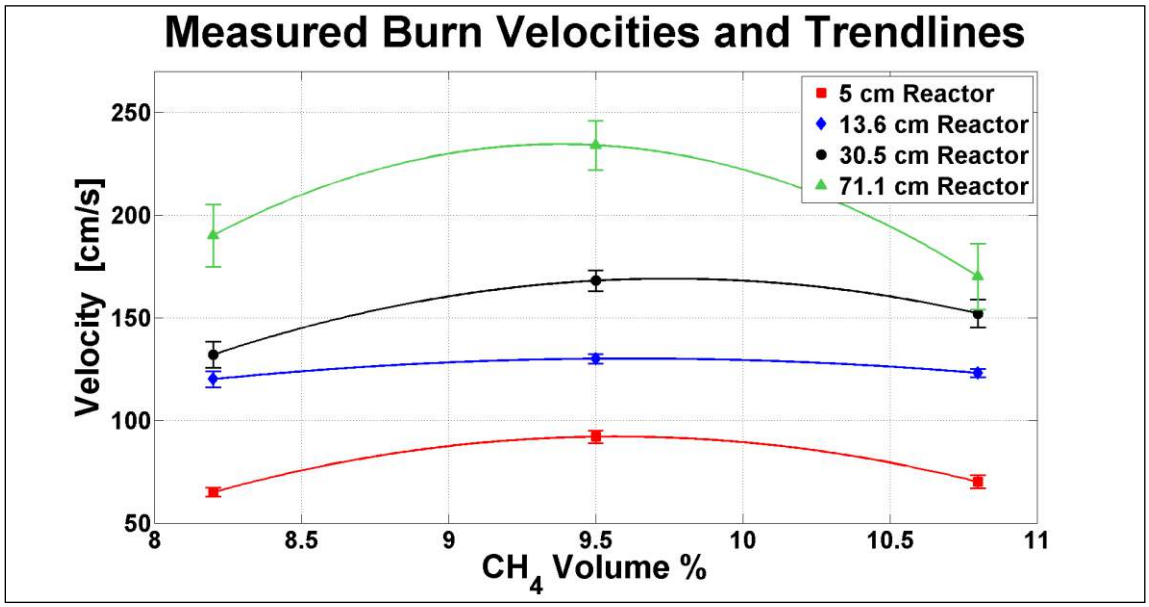

Figure 30. Flame velocity of the various reactor sizes. Tests were done 298 K and 81 kPa. Open-end ignition.

The goal of using various reactor sizes is to determine how the velocities will increase at the scale of a Longwall Gob. Initially velocity measurements were made using the 5, 13.6, and 30.5 cm reactor vessel, from this data an equation was obtained from a power law curve fit (correlation coefficient = 0.999) with the addition of data from a 2.5 cm reactor. Using this equation a prediction was made as to the burning velocity for a 71cm diameter reactor and then compared to actual measurements. It is extremely encouraging to see that having the multiple reactors allowed a trend to be observed and could predict the effect of increasing physical size of the reactor to within 3.4% for stoichiometric condition as seen below in Figure 31.

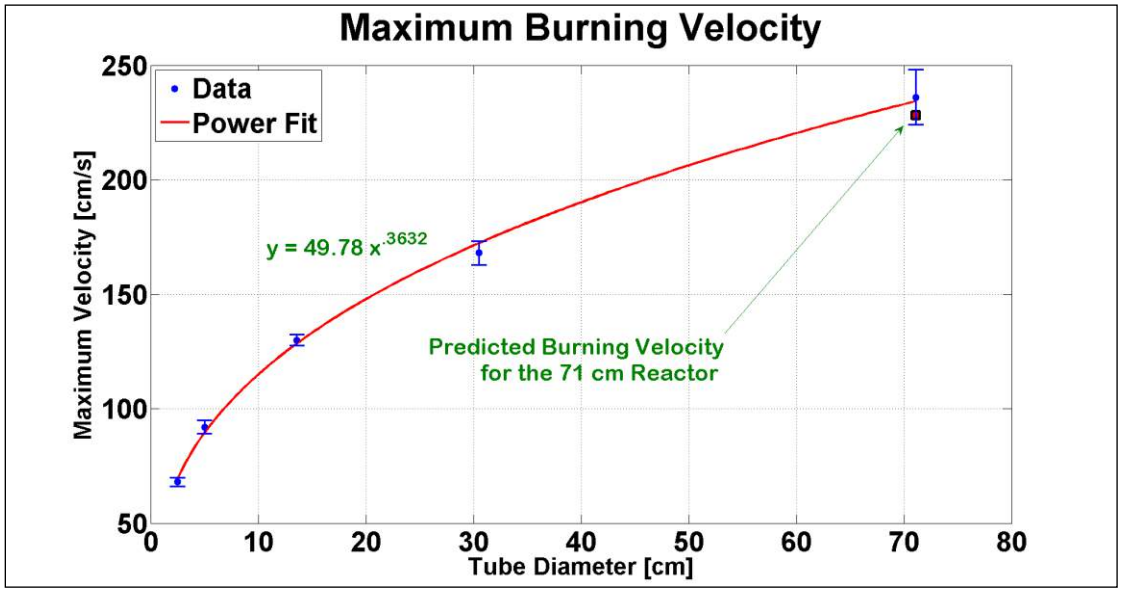

Figure 31. Curve fit including 71 cm reactor. The maximum uniform velocity is found near stoichiometric conditions in all cases. The conditions were 300 K and 81 kPa. Also shown is the value predicted by the curve fit as determine by the three small reactors.

The above results are obtained when the open end of the reactor was ignited. When the closed end of the reactor is ignited, the mixture begins with a laminar flame profile but rapidly accelerates and transitions to turbulence. This is a result of the expanding gasses behind the flame working to accelerate the flame as it travels, and no resistance upstream of the flame as seen when flame propagates to the closed end of the reactor. A series of measurements were made for methane-air mixtures at stoichiometric conditions. These measurements were made as near to the transition of the flame as possible before the flame became completely turbulent. The results are tabulated in Table 7. From the table it is seen how the build-up of pressure dramatically increases the speed of the flame. This becomes important in a large-scale explosion, especially one which occurs in a confined space, such as an underground mine. It is interesting to note that as the tube diameter increased, the effect of the pressure build up becomes more pronounced.

Table 7 Measured velocities [cm/s]. Stoichiometric ignition at ambient (300 K, 84 kPa) lab conditions.

Tube Diameter (cm)	Open End Ignition (cm/s)	Closed End Ignition (cm/s)
13.6	130	304
30.5	168	480
71.1	236	820

Task 1.2 – Methane flame propagation with simulated Gob

This task is focused on understanding the impact of simulated Gob properties on the flame interaction with the rock rubble. Based on theory and the observed burning velocities with the open and closed end ignition without rock rubble it was expected that the rock rubble would increase the burning velocities of the methane flame above the open end flame speeds, this is due to the increase in turbulent fluid motion and after the flame passing the rock rubble it acting as a porous wall resulting in similar behavior as the closed end ignition.

Task 1.2.1 – Simulated gob comparison with empty rector

Initial tests were conducted with a thin layer of rock rubble for the 13.5 cm quartz reactor and 30.5 cm steel reactor, with the thin layer rock rubble being 5.1 cm and 4.1 cm, respectively. Flame velocities at stoichiometric and lean conditions resulted in an increase in flame propagation velocities; however, the rich methane-air mixture produced an interesting result with a slower propagation velocity.

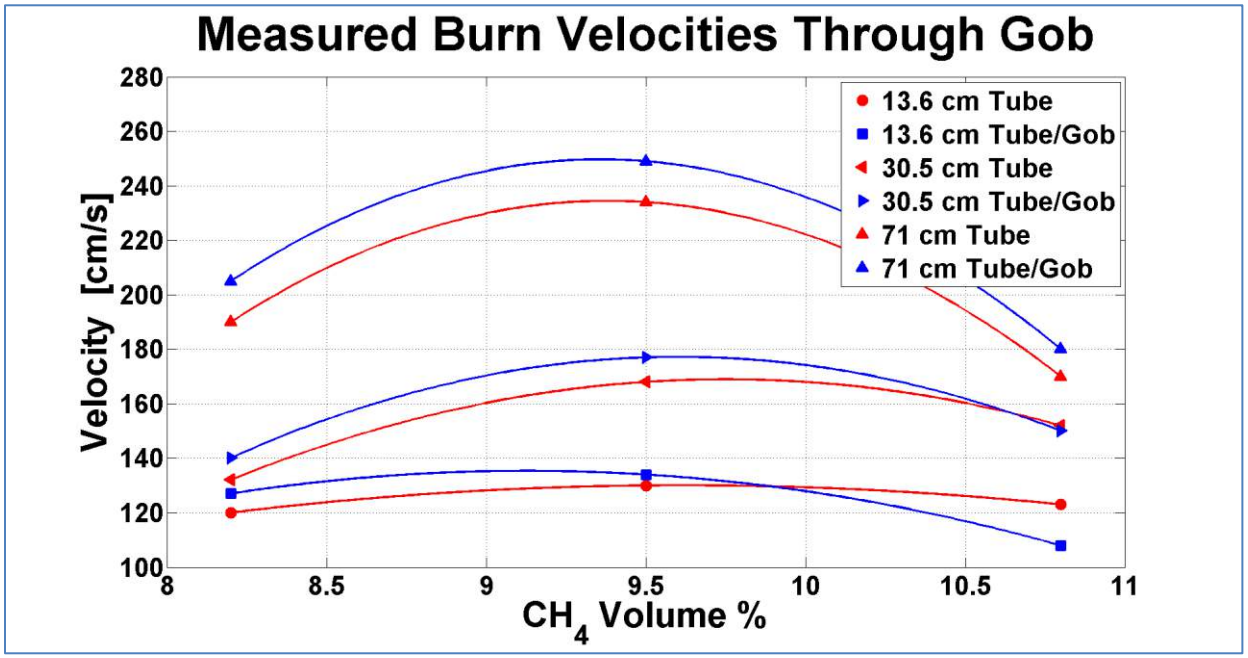

Figure 32. Comparison of methane flame velocities with a simulated Gob. Barrier lengths for the 13.5 quartz,30.5 steel and 71 cm steel reactors were 5.1cm, 4.1 cm and 20.2 cm, respectively.

Task 1.2.2 – Observation of complex flame interaction with rock rubble

Several tests were done with the 13.5 cm quartz reactor to observe the complex flame interaction with the rock rubble to provide additional information which could be utilized in the validation of the combustion model. Several major observations were seen from the high-speed imaging in the quartz reactor which has not previous been presented, see Figure 33.

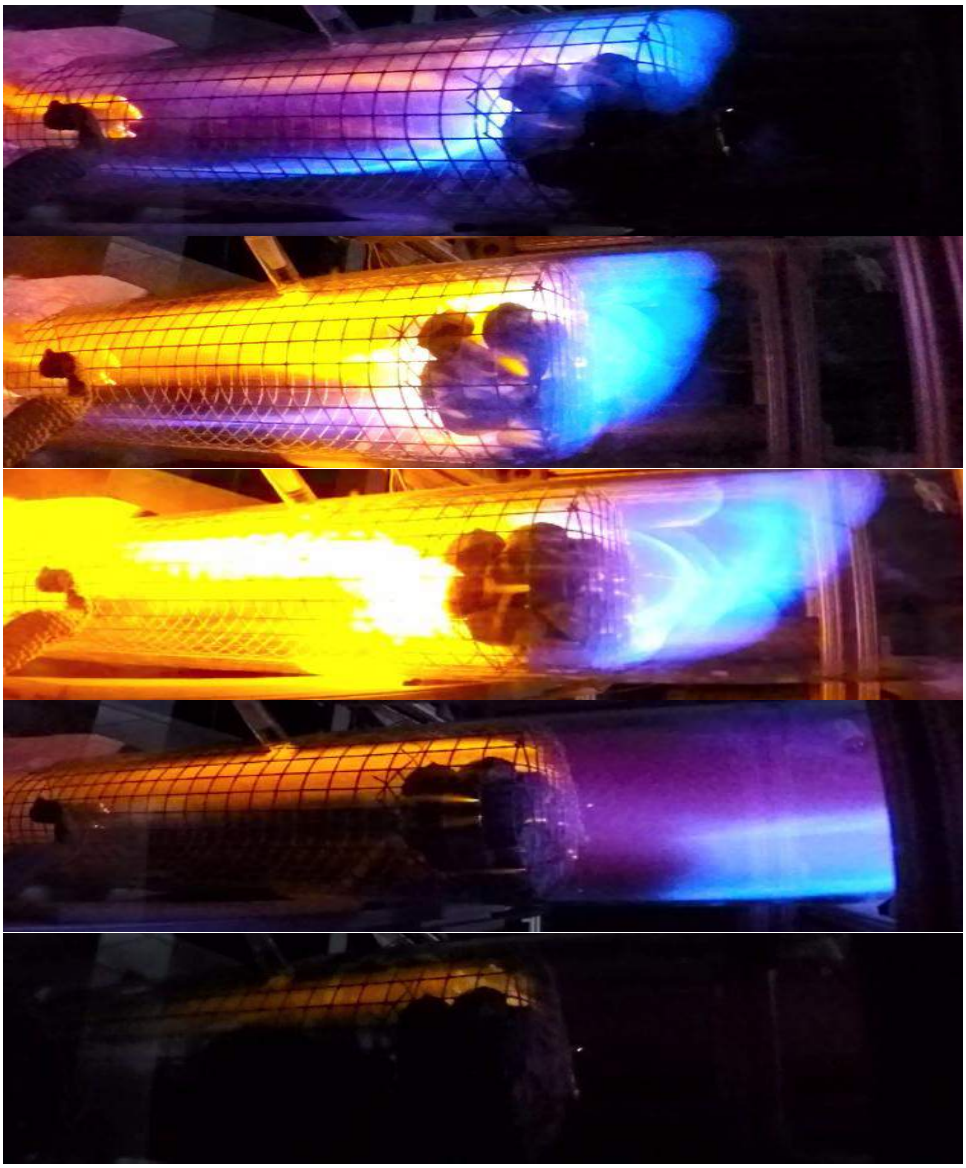

Figure 33. Methane flame interaction with rock rubble. This sequence of images shows the methane flame as it passes through the rock rubble in the 13.6 cm quartz tube. The top image shows the flame about to pass through to the back side of the rock rubble. The open end is seen on the left, where a soot rich region is seen in yellow-orange. The second and third images show the flame mostly past the rubble. Jets of burning exhaust gasses can be seen on the exhaust side of the rubble. Smaller jets of soot rich combustion streaks can be seen in the fourth and final images. These are believed to be areas of re-ignition as the hot exhaust gases interact with rich zones near the rocks.

Observations of the flame and rock rubble interactions as observed in the 13.5 cm quartz reactor show a large premixed blue flame passing through the void above the rock rubble which is proceeding at a faster velocity compared to the portion of the flame passing through the rock rubble. After the flame pass through the rock rubble, the hot products interacts with the rock dust and provides a bright yellow color which is indicative of black-body radiation which can also be seen by soot in a typical non-premixed flame or higher-hydrocarbon premixed flame. Another characteristic seen in the Figure above is small flame jets extruding from the voids between the rock rubble, this observation was also predicted by the combustion model as will be discussed in further detail later in the report.

Task 1.2.3 – Comparison of The effect of simulated Gob thickness on methane flame velocities

The barrier length of the rock rubble for the 13.5 cm quartz reactor, 30.5 cm steel reactor, and 71 cm reactor resulted in methane burning velocities increasing with increase in length of rock barrier at lean and stoichiometric conditions as seen below in Figure 34. This observation is important as it suggests that if the voids are sufficiently large to sustain a propagating flame this flame will transition to a fully turbulent propagating flame if burning lean or stoichiometrically. The reasoning for this reversal at rich methane-air conditions is currently under investigation and will be the focus of future research.

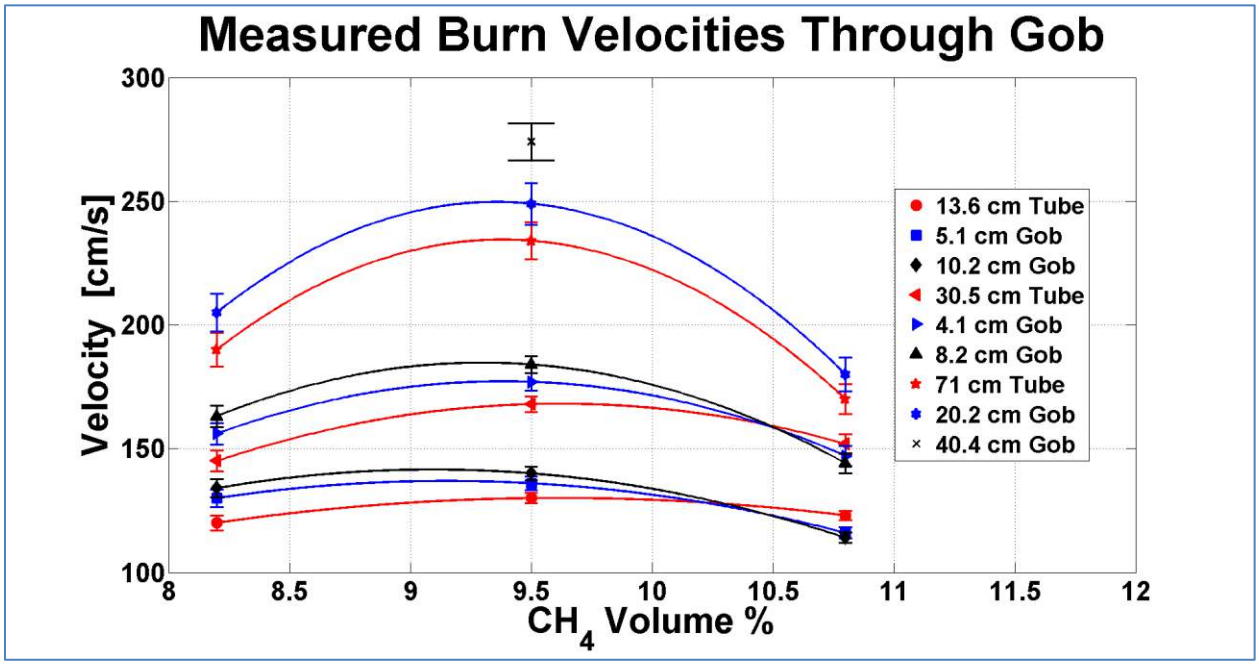

Figure 34. Increasing the barrier length of the rock rubble increased burning velocities for lean and stoichiometric conditions.

Task 1.2.4 – The effect of rock size in the simulated Gob on methane flame velocities

The size of rock was varied (2.8, 4, and 9 cm) while maintaining a constant barrier length of 9 cm. Interestingly, the largest rock size produced the largest burning velocity, while the mid-size rock produced the slowest burning velocity consistently across the methane-air mixtures investigated as shown below in Figure 35.

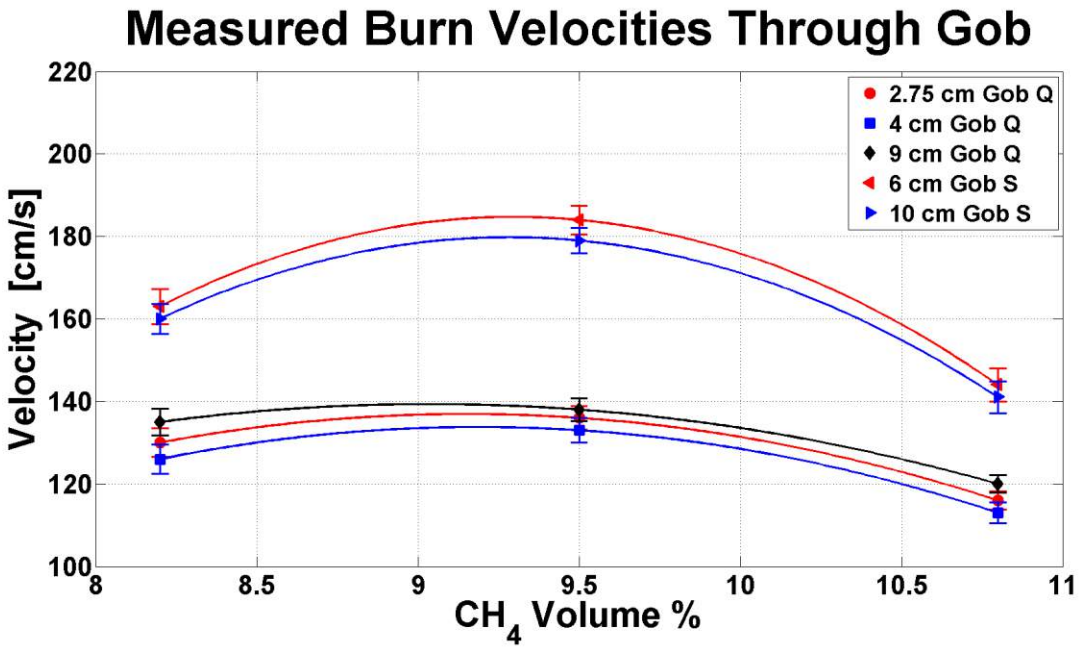

Figure 35. Varying the rock size produced a consistent trend across the various methane-air mixtures. This study was performed with marble in the 13.6 cm quartz reactor. Q = 13.6 cm Quartz, S = 30.5 cm high pressure steel reactor.

Task 1.2.5 – The effect of rock rubble barrier height on methane flame velocities

Variation in barrier height was investigated to determine the impact of allowing the rock rubble to have a void which is possible in the Longwall Gob area depending on the type of caving and compaction that occurred. Interestingly a 25% void space of the above the rock rubble seems to have little impact on the burning velocities once the flame passed the rock rubble, with the exception of the methane-air rich case as seen below in Figure 36. The closed end ignition is added for comparison and clearly shows a significant increase in burning velocities, which suggests that the rock rubble alone is sufficient for determining the full impact, but the location of the ignition will have a significant impact on the methane explosion.

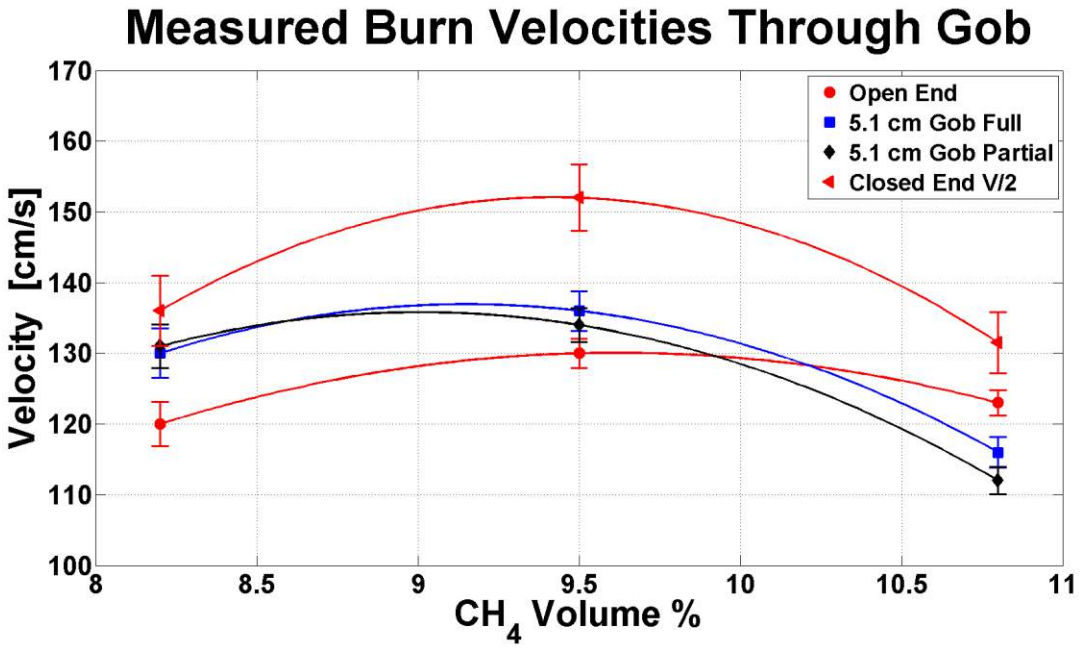

Figure 36. Impact of barrier height on methane burning velocities. The effect of barrier height on burning velocity. The partial barrier is about 3/4 the diameter of the reactor.

Task 1.2.6 – The effect of humidity on methane flame velocities in simulated Gob

The impact of humidity on methane burning velocities was investigated, due to the possibility of have varying ambient conditions in the Longwall Gob area with respect to moisture levels in the air and possibly the rock rubble. The relative humidity was increased from 10% to 16% in both the 13.5 cm quartz reactor and 30.5 cm steel reactor, both resulting in a reduction in methane burning velocities at the lean and stoichiometric case with less of an impact for the methane-air rich case as seen in Figure 37.

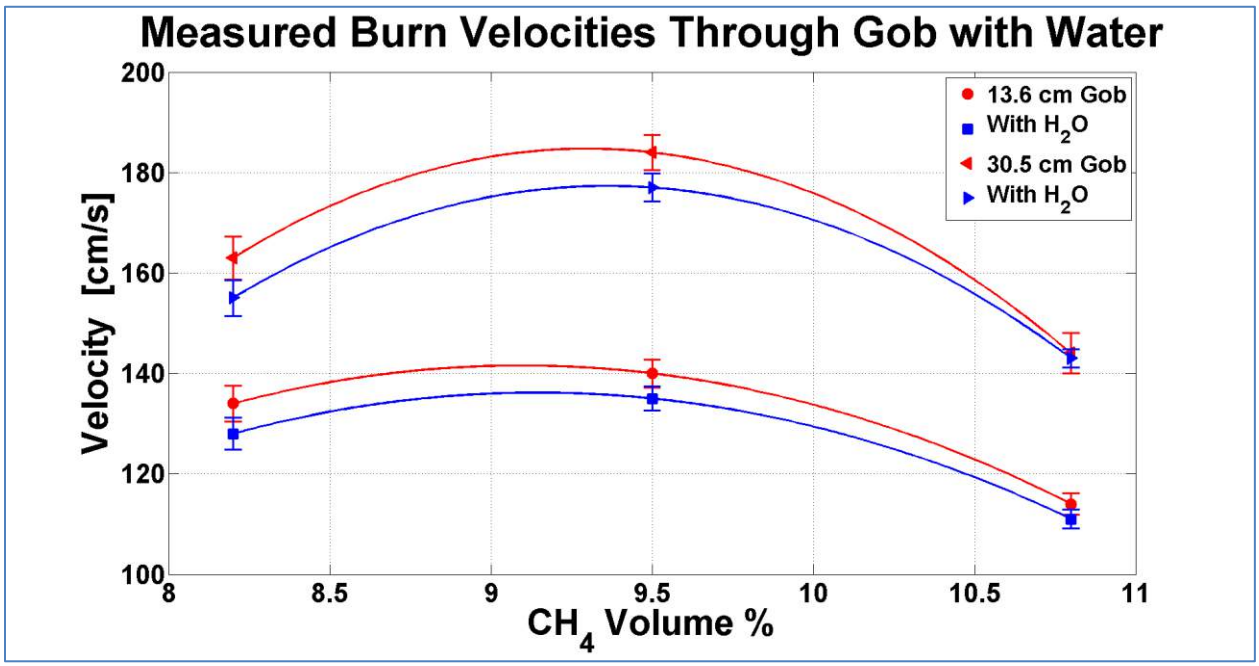

Figure 37. Increasing the moisture levels of the ambient air reduced the burning velocity. Barrier lengths for the 13.6 cm quartz and 30.5 cm steel reactor was 5.1cm and 4.1 cm, respectively. The rock sizes for the 13.6 cm quartz and 30.5 cm steel reactor was 2.7 cm and 6.5 cm, respectively.

Task 1.2.7 – The effect of various rock material on methane flame velocities

It is known that the rock material in the Longwall Gob area varies depending on location and overburden. Thus, it is important to try to characterize the impact rock material properties, and physical features may have on the burning velocities as this will allow the various mines to tailor the a predictive model based on information about the rock rubble in the Gob area. The rock rubble in these tests was changed from the solid smooth River Rock (Granite) to Lava Rocks (Basalt) which are more porous and rough edges. The Lava Rock resulted in a slight increase compared to the River Rock at stoichiometric conditions, but additional tests are required to determine if there are sufficient statistical differences based on the error bars as see below in Figure 38.

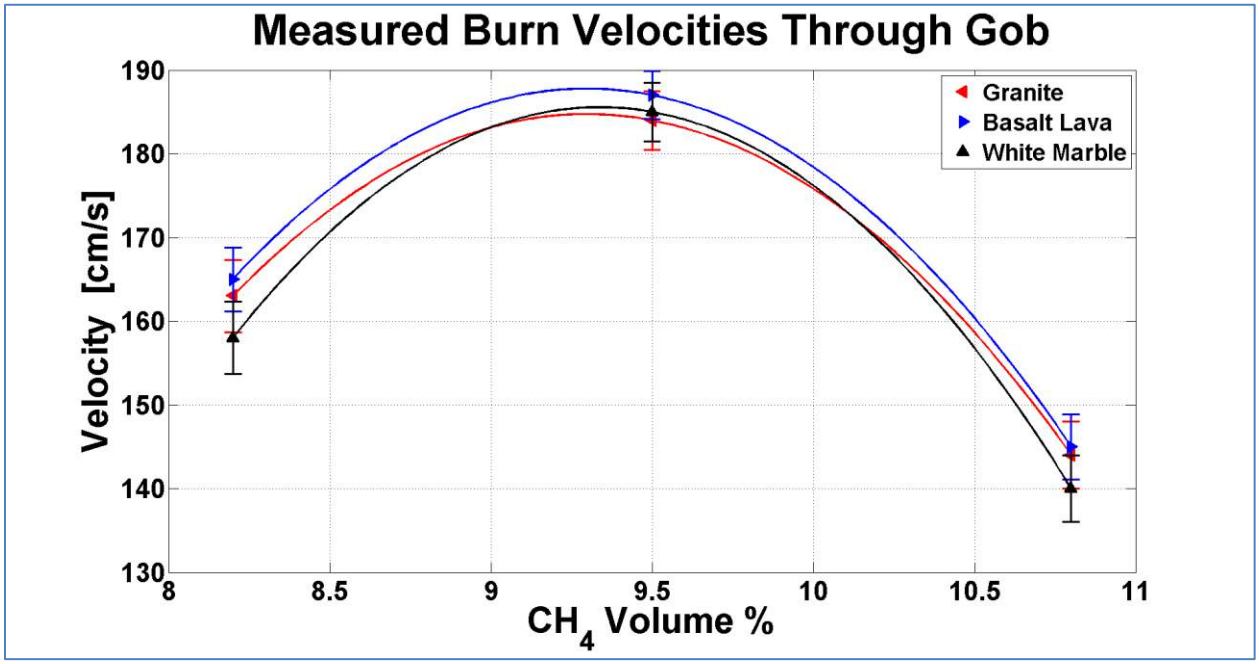

Figure 38. The effect of rock material on methane burning velocities. The basalt lava is highly porous compared to the granite rock.

Task 1.2.8 – The effect of rock rubble temperature on methane

The effect of rock rubble temperature on burning velocities was investigated; as the potential for localized temperature increases in the Longwall Gob are may be possible from exothermic heating from coal. The low thermal conductivity of the rocks cause them to retain a lot of the heat and thus heating the methane-air mixture which in turns increases the flame speed since it is extremely sensitive to temperature as was seen in Figure 39. Increase in Gob temperature above 50°C resulted in a significant increase in flame velocities.

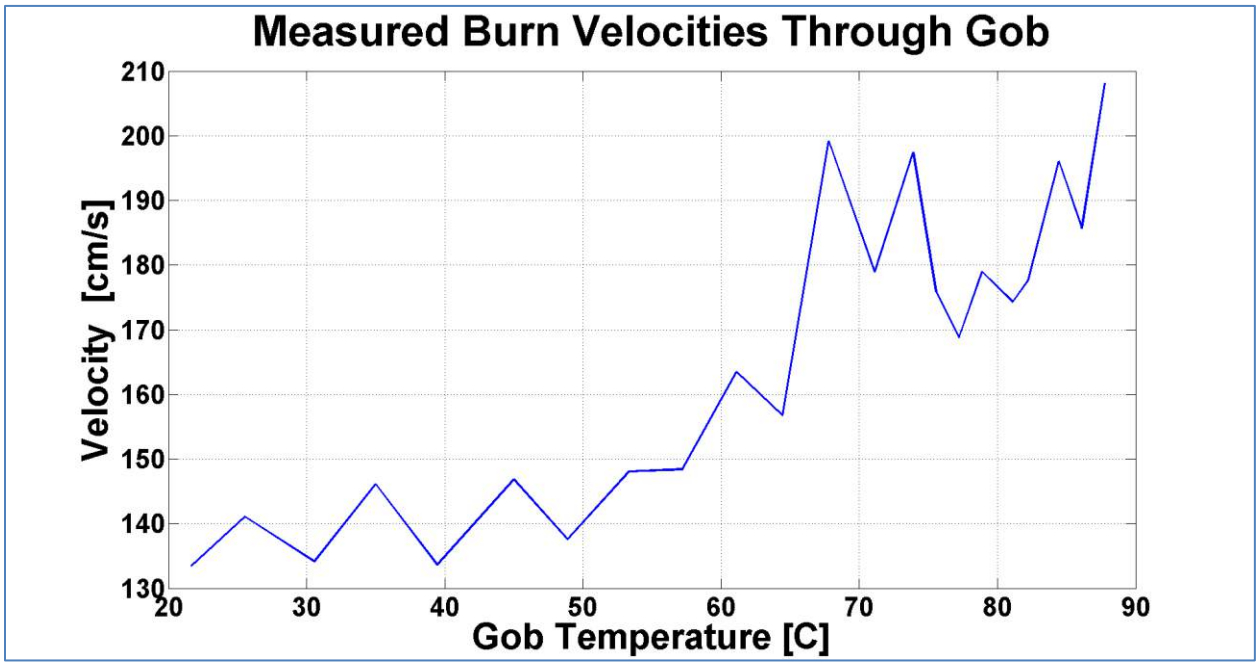

Figure 39. Impact of Gob temperatures on methane burning velocities as measured in the 13.6 cm quartz reactor. Stoichiometric conditions.

Task 1.3 – Key findings and insights from experiments

These major discoveries and insights are important for model validation and some will require additional research to try to gain a better understanding of the underlining principles and/or coupling of the complex interactions of the flame and rock rubble.

- After flame pass through and over rock rubble, portion of unburned gas mix with hot products and interacts with the hot rock and causes a re-ignition event. This observation was not predicted or expected.
- As the flame passes through the rock rubble, small jets of ignition events are observed from the voids between the rock rubble.
- Rich methane-air flames have a slower burning velocity within the simulate Gob tests compared to faster burning velocities for lean and stoichiometric conditions.
- With barrier length fixed in the 13.5 cm quartz reactor, the largest rock size (9 cm) produced the largest burning velocity, while the mid-size rock (4 cm) produced the slowest burning velocity and the smallest rock (2.5 cm) producing the mid-range burning velocities consistently across the methane-air.
- The effect of increasing the water vapor concentration appears to be to lower the burning velocities through the Gob material. This is expected based on theoretical considerations. For example, more water means less combustible mixture volume and a larger mixture heat capacity. This larger heat capacity may be acting to slow the kinetics down through heat absorption.
- The effect of Gob temperature is to increase the burning velocity through the Gob. This is likely due to the higher temperatures advantaging kinetic rates near the rocks surface.
- A difference between porous rock rubble and nonporous is also apparent. The porous material may be able to harbor an ignitable quantity of methane-air mixture as the flame passes. The pores may also increase local turbulence.

Task 2 Comparison of combustion model with experimental results

Task 2.1 – Model of flame reactor no simulated Gob

In Figure 40 the beginnings of the buoyancy driven asymmetry can be seen. The hotter gasses rise behind the flame, as shown in the contour plot of density. It is this buoyancy that gives the developed flame its asymmetric profile (see the experimental section for images). Without this effect, the shape of the flame would remain symmetric as it appears in the initial stages.

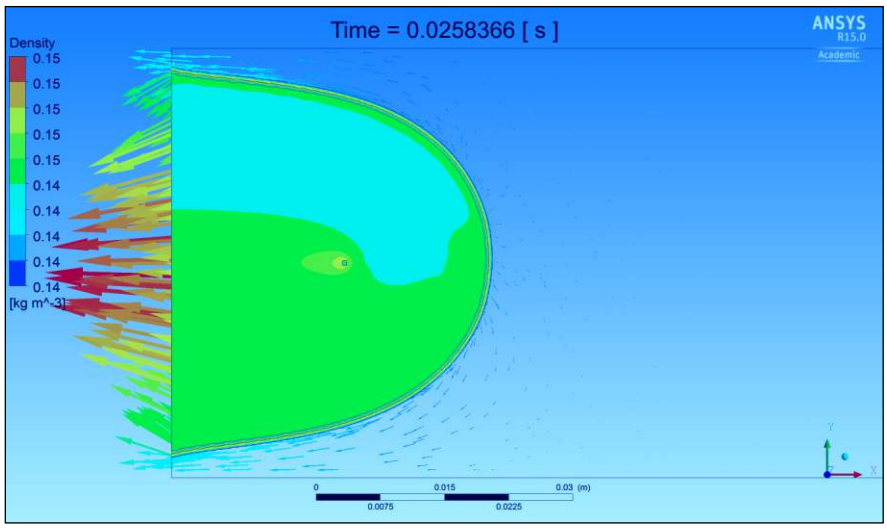

Figure 40. Density contour behind the flame. Note the less dense gasses on top. All simulations were done with standard laboratory conditions. This is stoichiometric methane in air.

The ANSYS model was used to calculate the propagation velocities for tubes of diameters 5 cm, 13.6 cm and 30 cm. To determine these velocities, the distance traveled by the uniform flame along a line parallel to the cylinder axis was divided by the calculated travel time, as would be measured by stationary flame detectors in an actual tube. The predicted velocities at stoichiometric conditions were subjected to a power law curve fit, shown in figure 41. This fit has a correlation coefficient of .9988. A comparison with the experimental values shows that the ANSYS model predictions follow a similar pattern but with much slower growth as a function of tube increase. This makes sense because the area of a plane channel grows linearly with increasing channel height, while the area of the tube cross-section grows quadratically with diameter.

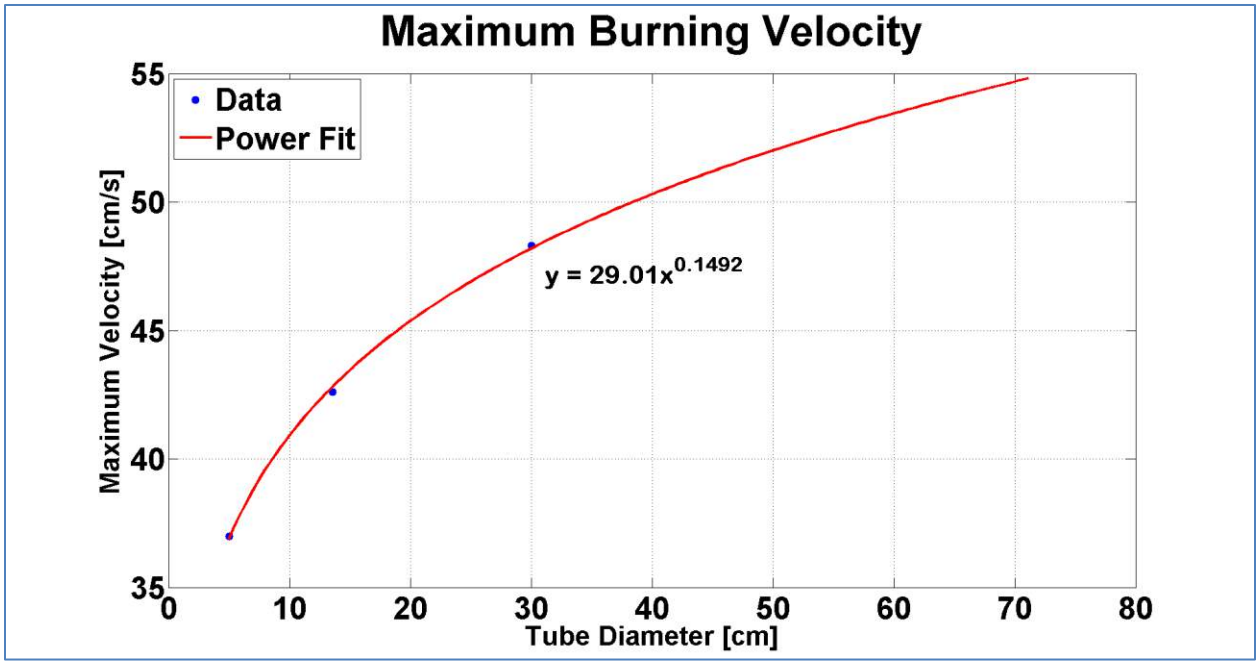

Figure 41. Propagation velocity of ANSYS 2D model. The maximum uniform velocity is found near stoichiometric conditions in all cases. The conditions were 300 K and 101 kPa.

Improvements to the model will include the use of 3-D geometry. Though it is computationally more expensive, the geometric effects on the predicted burning velocities values will only improve with a more accurate geometry. Additionally, other boundary conditions and values will be explored. These effects are important because the removal of heat from the flame at the boundary will impact the kinetic rate in the near field. Refinements to the current model will incorporate more individual values for external emissivity and tube wall conductivity.

Figure 42 shows a deflagration simulation traveling along a 5 cm planer tube, further developed than the initial flames in the previous two images. The shape of the flame should be compared to the experimental images found in the experimental section. This shape is due to buoyancy effects. As the burned gasses expand behind the flame, they tend to rise and push the top part of the flame towards the unburned gasses, while leaving the lower edge trailing.

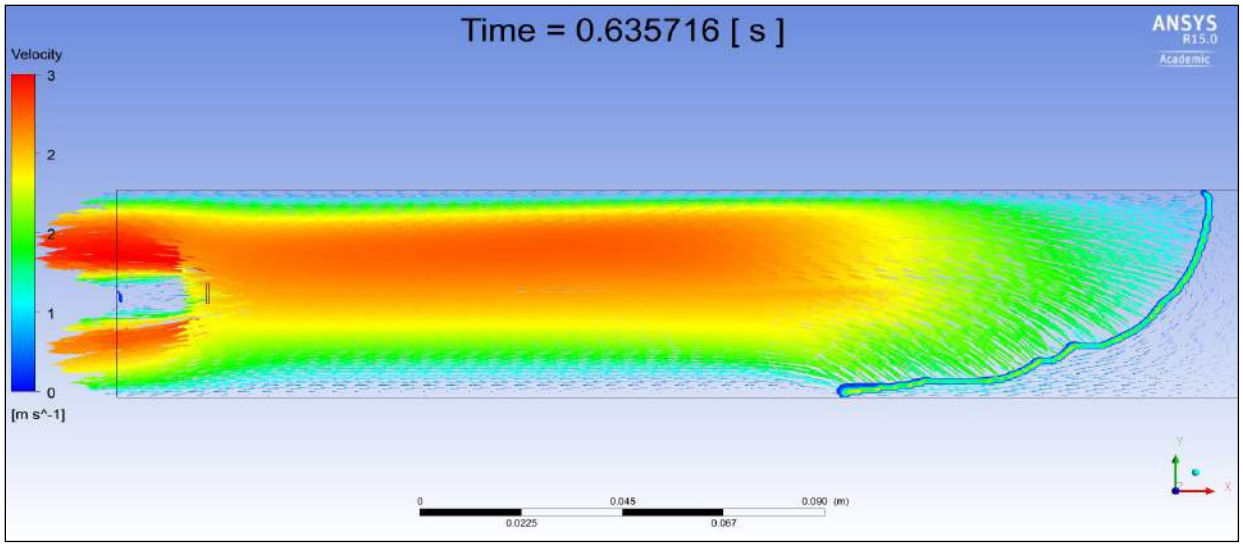

Figure 42. Here the flame is traveling to the right, with velocity direction arrows pointed to the left. Note in the region behind the flame the velocities are higher than in the front, as indicated by the relative sizes of the arrows. Also note the gas flow around the rectangular igniting wall near the outlet on the left.

Task 2.2 – Interaction of propagating flame with simulated Gob (i.e. circular rock rubble)

The process of flames traveling through obstacles was modeled in the planer flame model by placing round objects in the path of the flame. As in the experiment, the flame appears to easily pass through when 2mm spacing is used. These results are shown in Figures 43 – 45 below. These are adiabatic walls. Velocity jets between the obstacles agree with the high temperature flame jets seen experimentally in the quartz reactor.

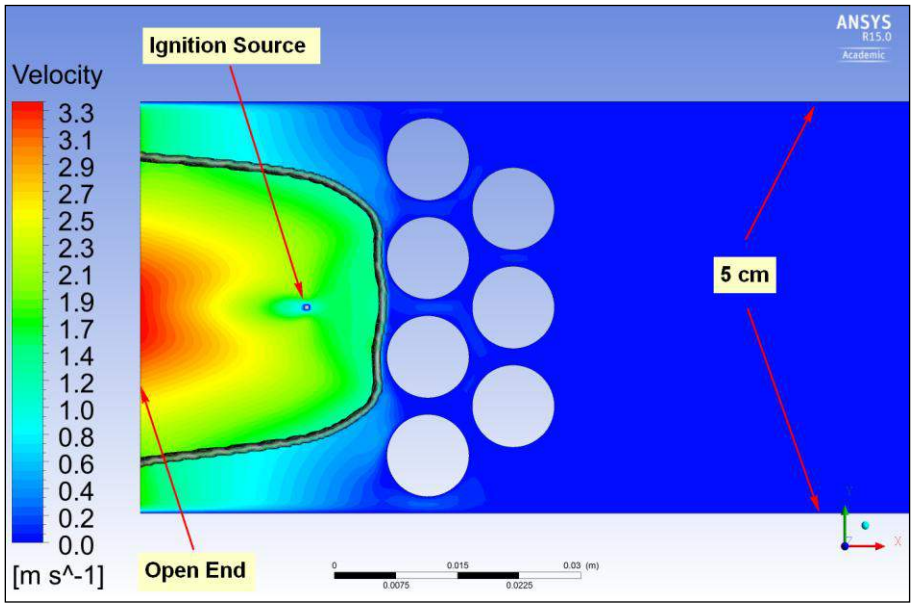

Figure 43. Flame approaching obstacles. Obstacles are 1 cm in diameter. Stoichiometric methane-air mixtures ignited at standard laboratory conditions of 300 K and 101 kPa.

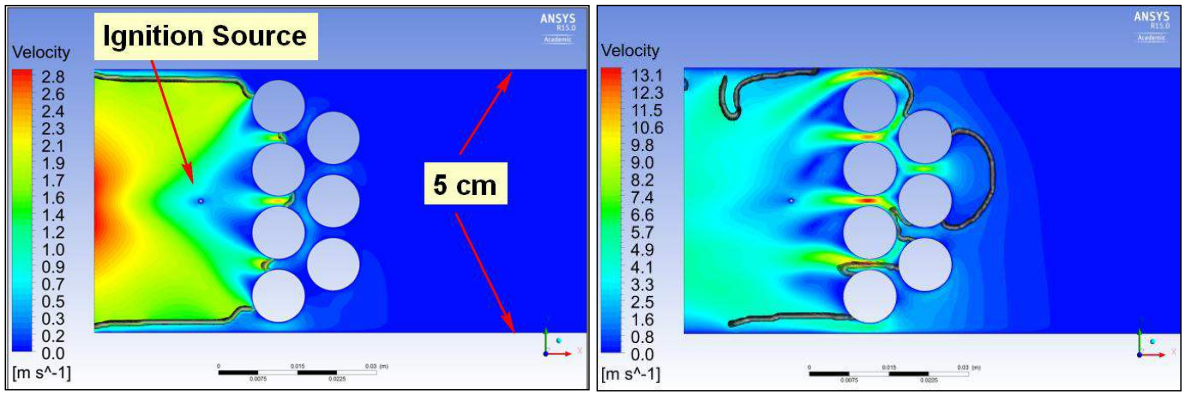

Figure 44. Flame contacts and penetrates obstacles. Stoichiometric methane-air mixtures ignited at standard laboratory conditions of 300 K and 101 kPa

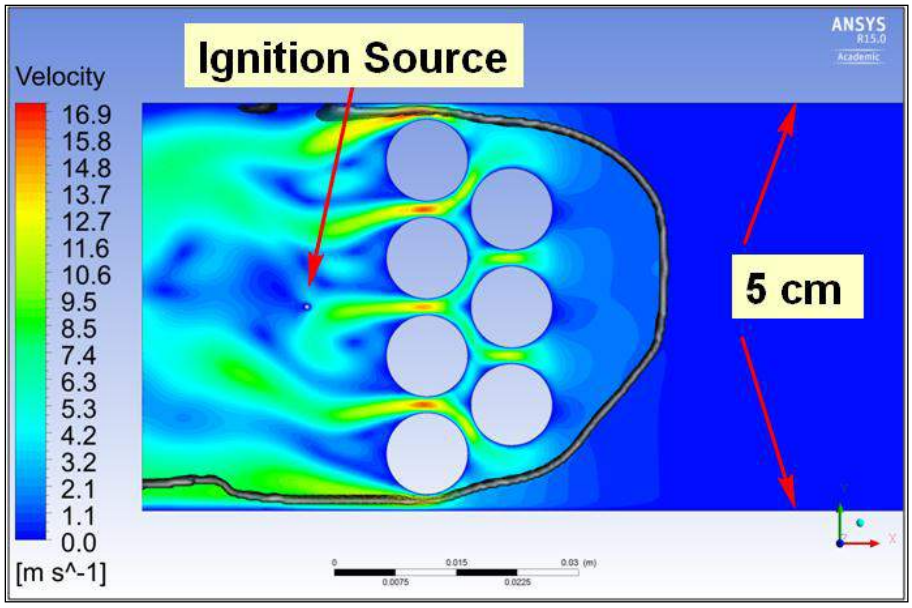

Figure 45. Flame moving into mixture past obstacles. Stoichiometric methane-air mixtures ignited at standard laboratory conditions of 300 K and 101 kPa.

Another model was made with more rows of adiabatic obstacles to examine the effects of more resistance to flow. It can be seen that the thicker layer of obstacles results in a slightly lower velocity of the exhaust gasses through the layer as seen in Figure 44.

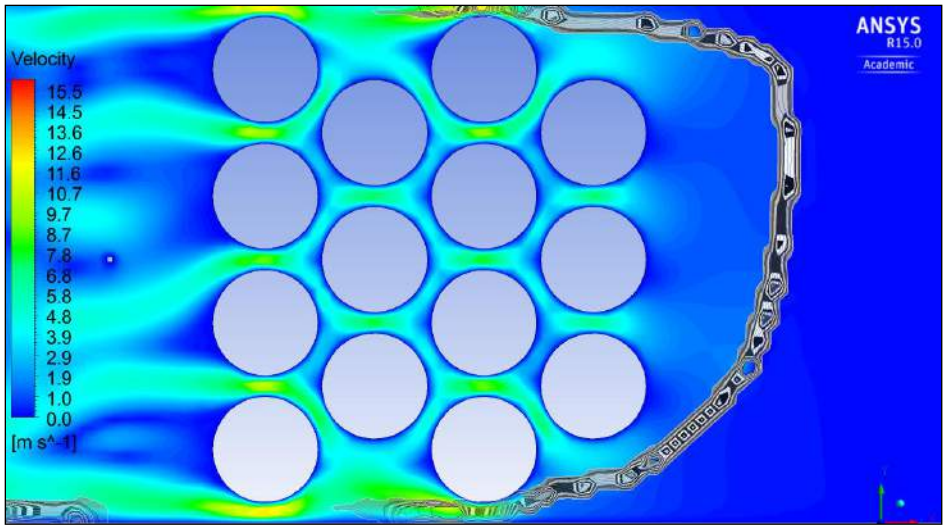

Figure 46. Velocity profile after flame passes. Loss is due to no slip conditions at boundaries of obstacles. The flame is shown with black-and-white contours.

The effect of smaller adiabatic obstacles with non-uniform spacing was then examined. Here 2 mm spheres were used, and space was left around the pile for venting. As expected, large gas streams are seen leaving around the edges of the obstacles as seen in Figure 47.

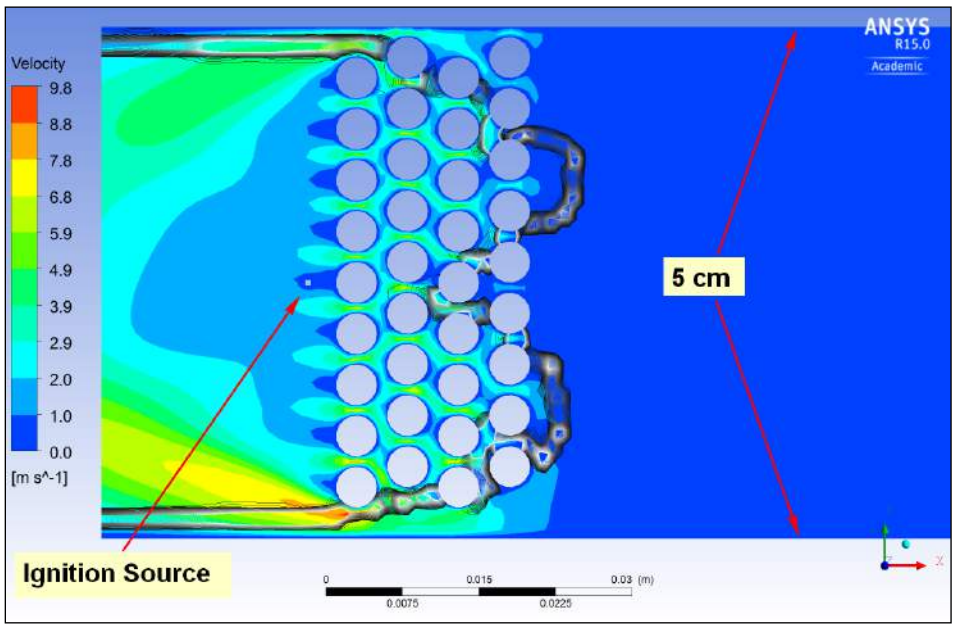

Figure 47. Smaller adiabatic obstacles with non-uniform spacing. Stoichiometric methane-air mixtures ignited at standard laboratory conditions of 300 K and 101 kPa.

Finally, a model was run with the smaller obstacles but this time the boundary conditions were not adiabatic. A constant temperature of 300 K was chosen for the obstacles. The results show only a slight difference in velocity profile compared to the adiabatic case.

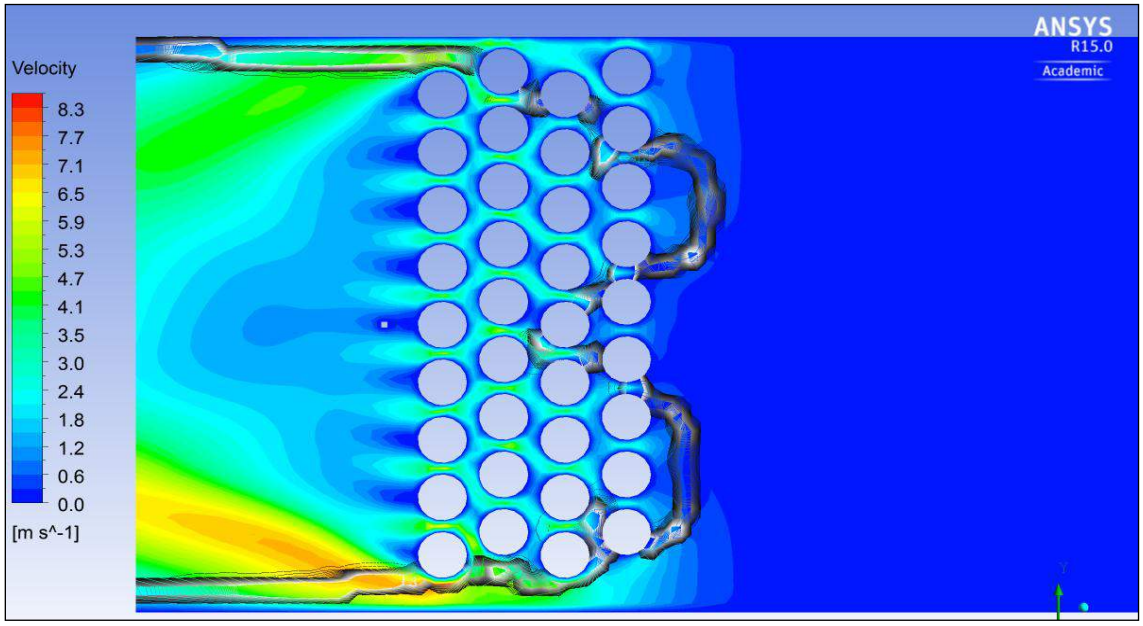

Figure 48. Same model parameters as in Figure 47, except that the obstacles were kept at a constant temperature of 300 K.

Task 2.2 – Predicted trends

The models built to simulate a methane flame passing through Gob-like structures predict pressure rises and increases in burning velocities due to turbulence and back pressure. Different rock sizes have only a minor effect on model results, at least for the small variations modeled so far. The presence of water also shows slower velocities for stoichiometric conditions on the order of 4% reduction for 10% water vapor. Predicted values for models of the 13.6 cm reactor and the 30.5 cm reactor are tabulated below, along with experimental results for comparison. The simulation used many of the experimental results show little differences of burning velocities or pressure rises, and so these were not modeled.

Table 8. Comparison of model and experimental results due to the impact of simulated gob

Reactors	*Pressure Rise behind gob(%)*	*Burning Velocity increase due to gob(%)*
Experimental 13.6 diameter	*8.5*	*3.7*
Model 13.6 diameter	*3.1*	*3.9*
Experimental 30.5 diameter	*10*	*5.6*
Model 30.5 diameter	*3.2*	*4.3*

Task 2.3 – Key findings and insights from the combustion model with simulated Gob

- Jets occurred between rock rubble as observed in the experimental section. The velocity of these jets is related to the spacing and thickness of the rubble. As expected, the thicker the plug the more resistance to flow in the plug, and also the larger pressures achieved.
- The dampening effects of water vapor can be captured. This is important because water may help serve an important mitigating factor in future ventilation systems.
- Impact of rock rubble size is minimal for the size ranges modeled. Rock size seems to be important only as it is related to spacing thickness.
- Rubble thickness does serve to increase pressure on the backside of the Gob.

Task 3 – Integration of combustion model into three dimensional CFD model of Longwall coal mine U-type ventilation system

Task 3.1 - Tracking and coupling chemical reaction (small scale) and fluid motion (large scale) during a transient analysis

The presence of EGZs in the tailgate and in the first two shields from the tailgate can be seen in Figure 49. The white circles are cross-sections of the hydraulic roof jack supports and the white ovals represent cross-sections of the jack hinge supports (See figure 50 for details).

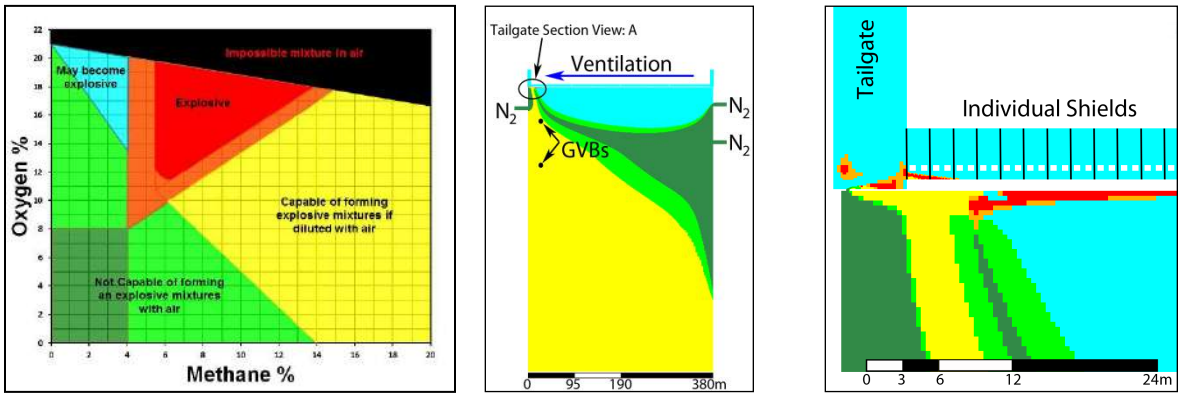

Figure 49 (L) Coward's triangle, showing the color key for the other two images. (M) Explosive gas zone (EGZ) plot of a progressively sealed Gob using U-type Ventilation. (R) Detail of tailgate section, near shields.

In order to model the chemistry of combustion of a methane-air mixture a scaling of this large mine ventilation models is required, which has approximately 9 million cells. The data from the model as shown in Figure 49 is first interpolated to a more detailed model and mesh of the tailgate and the first 20 shields. Figure 50 shows a detailed view of the mesh of the shields. The flow conditions at the boundaries are exported as profiles and used a constant inlet velocity, pressure inlet, or pressure outlet with the associated species concentration. The model is then solved to convergence in a steady-state simulation to resolve any geometry mismatches between the large ventilation model, which used only hexahedron cells and right angles, and the more detail tetrahedron mesh of the shields.

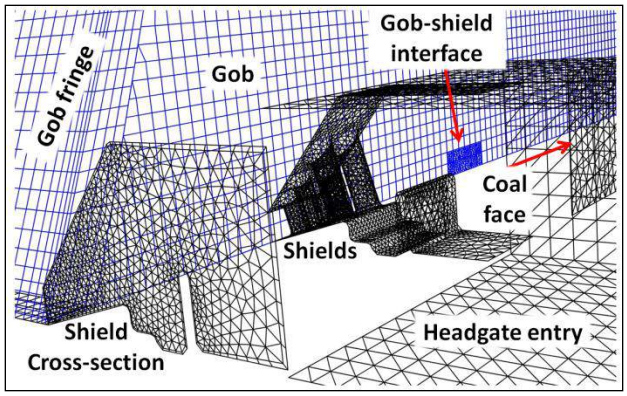

Figure 50. Mesh of the longwall face and Gob area directly behind the shields.

Figure 51 shows the EGZ using the newly converged model. The EGZ has changed in size, but the resolution of the shields has significantly increased. The model is once again simplified to a single shield. Figure 51 also shows the selected ignition location with a molar concentration of oxygen of 15.5% and a molar concentration of methane of 8.9% located on a plane 1-meter above the mine floor. This initial location was chosen due to some convergence issues which were not fully resolved, prior to the end of the project with the location of the ignition source within the gob area. However, the impact of the gob area behind the shields still have an impact on the pressure and flame propagation and along with the obstacles caused by the roof jacks and hinge supports causes the deflagration flame to become supersonic. Moving the location of the ignition source to the other EGZ (Figure 49) further into the gob behind the shields is currently underway.

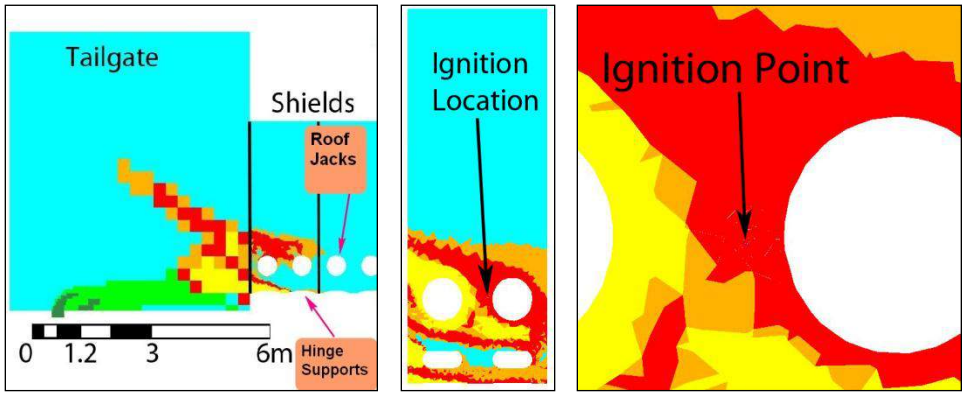

Figure 51. EGZ using a more detailed model of the shields and tailgate. EGZ at 1 meter above the mine floor and location of ignition point. This is a close-up of the same tailgate section shown above. The roof jacks are shown as white circles and are 0.5 meters in diameter. The hinge supports are shown as white ovals in the middle plot.

Figure 52 shows a closer view of the ignition point at a simulation time of 0.0025 milliseconds where the cell volume ranges from 10 $x^{-12}m^3$ to $10x10^{-14}m^3$, and the flame reaction zone is shown in red with a radius of 2 mm. The cell volume of a tetrahedral cell must be on the order of $10x10^{-14}m^3$ to have 5 to 10 cells across the flame after accounting for possible skewness. This

ensures that the cell edge size in the pre-heat and reaction zone will have a dimension an order of magnitude less than the flame thickness.

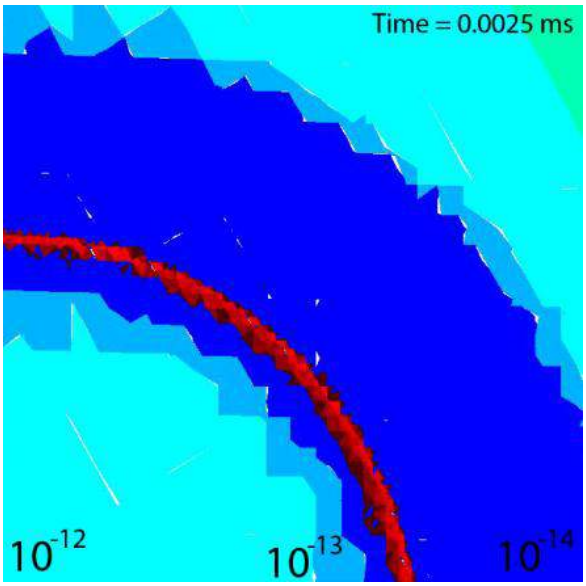

Figure 52. Flame front. Cell volume and reaction zone (flame). The thin red band is the spreading flame. Note that grid adaption has taken place, and that the smallest cells surround the flame.

Of primary importance from a safety standpoint are the flame regime (laminar, turbulent or detonation) and pressure increases associated with an explosion in a mine. Shown in Figure 53 is the initial progression of the flame as it increases to turbulent and nears detonation velocities.

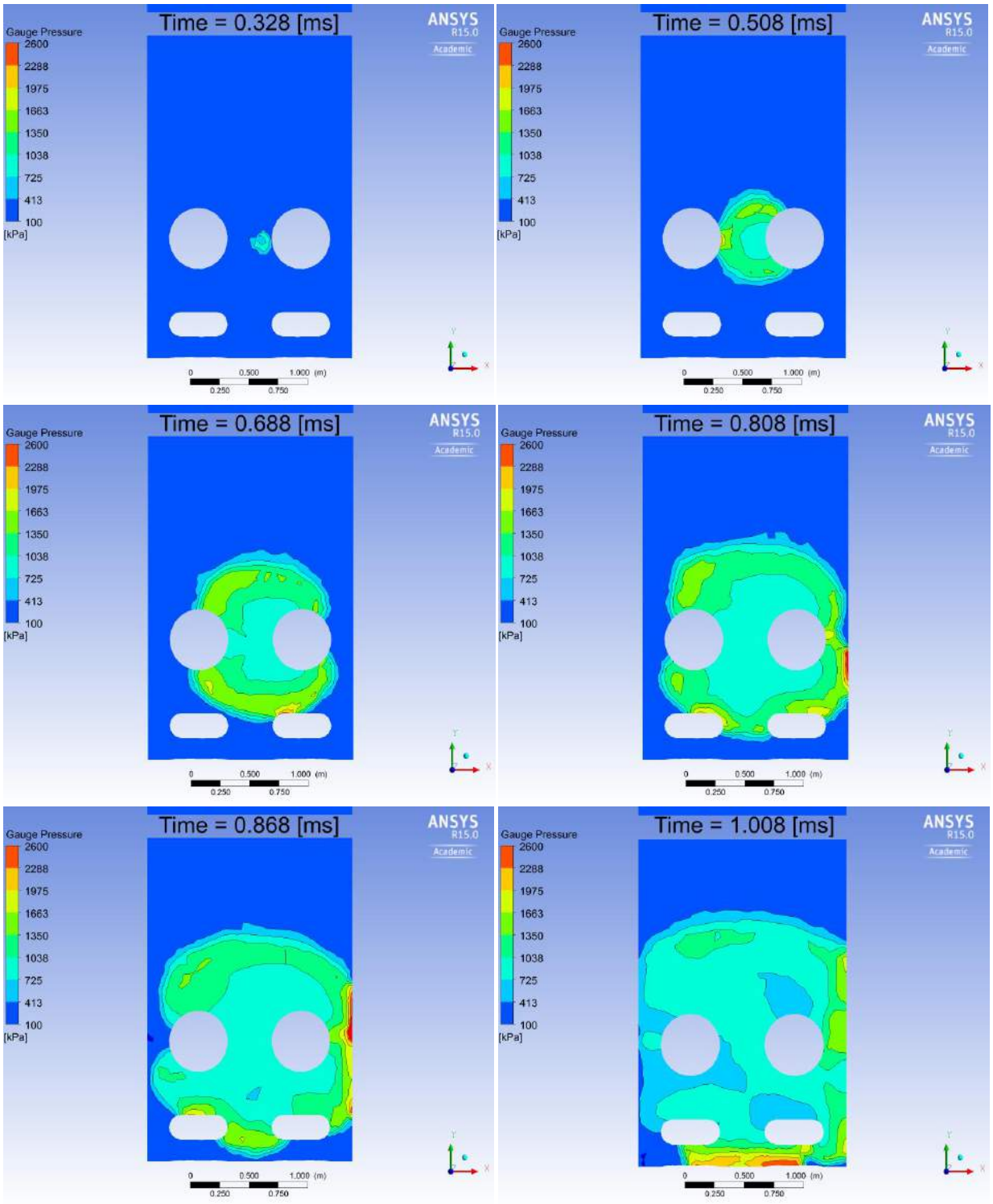

Figure 53. Sequence showing the increase in pressure as the methane explosion passes the shield columns near the tailgate. The pressures are largest where the flame has contacted structures.

Figure 54 shows the burning velocity as the explosion progresses. As can be seen, the flame speeds up into the turbulent and even detonation velocities range. Preliminary results indicate

that this flame will continue to speed up. Since the combustion model has been shown to handle detonations on smaller scale models, it is expected that as the flame continues to increase in velocity, detonation characteristics could be captured.

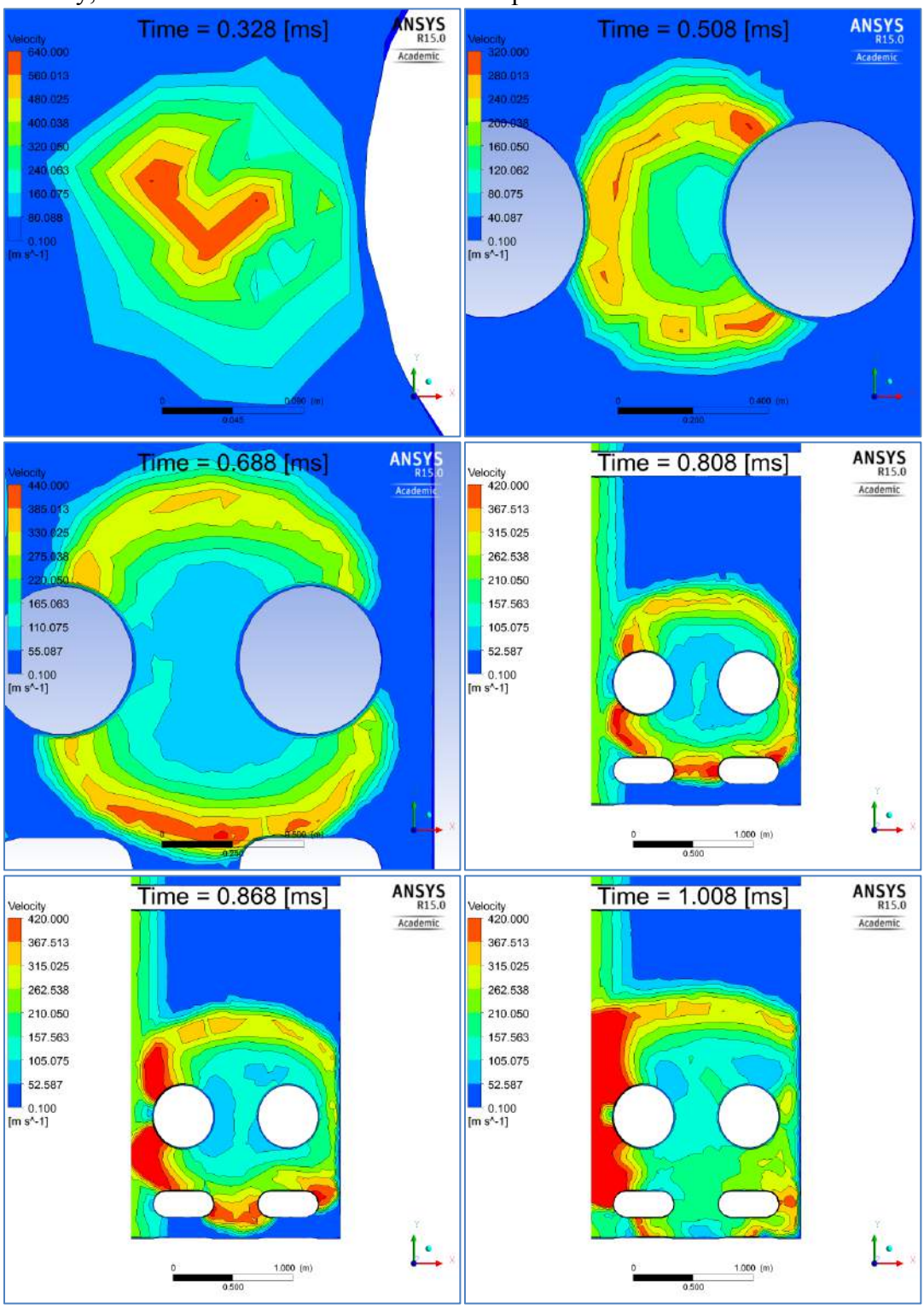

Figure 54. Velocity increases as the flame advances through the shields area near the tailgate and becomes supersonic.

Next steps with the large model integration involved moving the ignition point further into the gob (2073 m from the face) for a Bleedered-ventilated Gob as shown below in Figure 55.

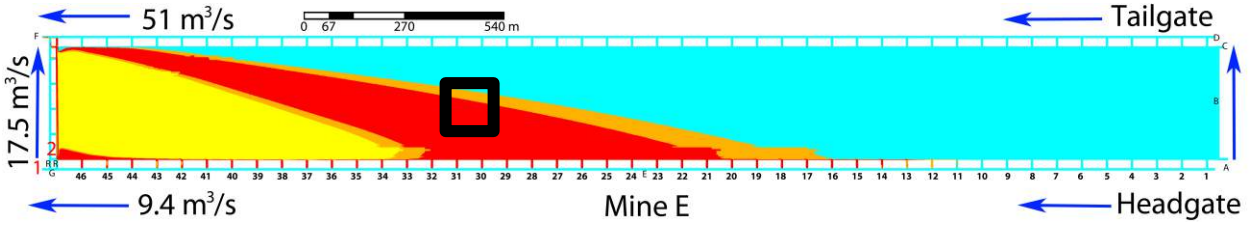

Figure 55. Bleeder-ventilated Gob showing location of the ignition source in the black square.

The location surrounding the ignition event located in the black square as identified in Figure 55, had significant refinement done to capture the thin reaction zone as shown below in Figure 56.

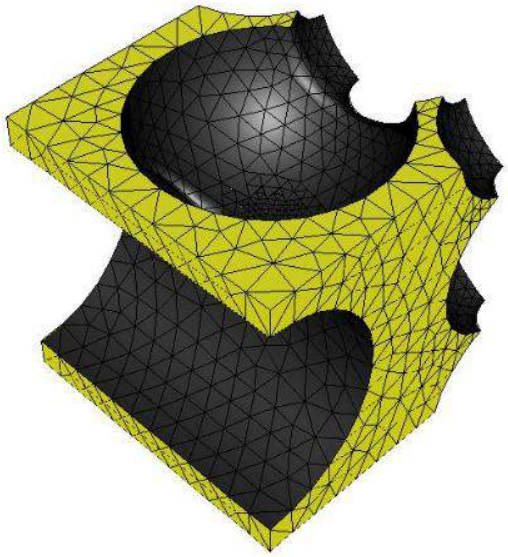

Figure 56. 1m cube fluid domain mesh with estimated porosity of 46%

After refinement of the fluid domain to capture the thin reaction zone, a spark was initiated with a sphere of 1.5 mm. Further back in the gob with less porosity the flame development does not occur as rapidly as shown earlier when the ignition event is located between the shields and the turbulent flow increases transport and allows for a faster transition. Further back in the gob, the velocity of the flame growth is only 1.23 m/s at approximately 1.8 ms as shown below in Figure 57 and 58; this is compared to the detonation velocity of 420 m/s at 1.0 ms as seen earlier in Figure 54.

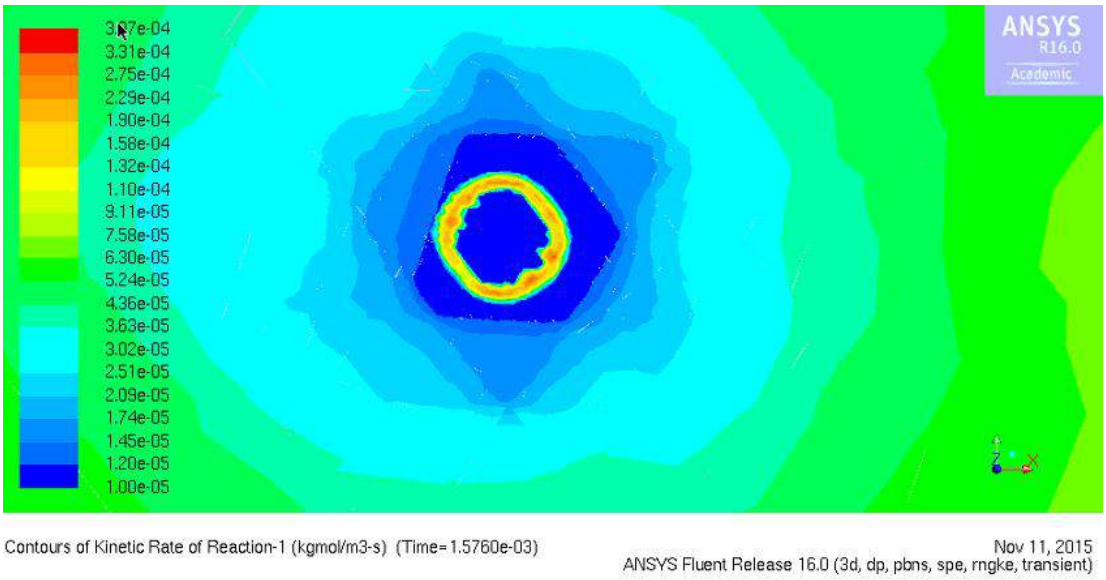

Figure 57. Reaction zone for flame development further into the gob at ~1.6 ms. Growth velocity 0.92 m/s

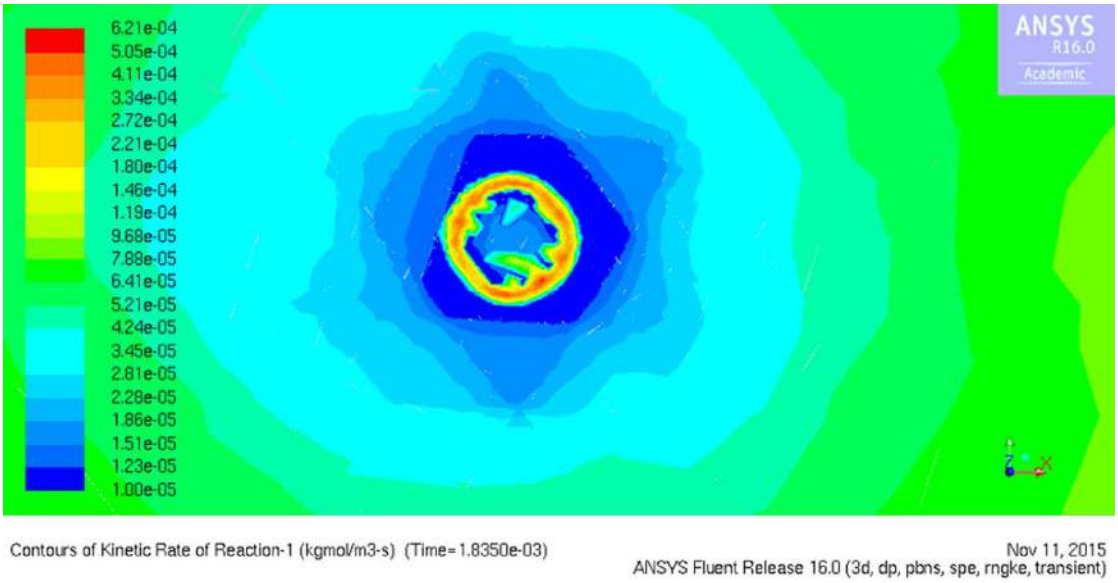

Figure 58. Reaction zone for flame development further into the gob at ~1.8ms. Growth velocity is 1.23 m/s.

Task 3.1 – Key findings and insights from the fully coupled three dimensional model

- The fully coupled three dimension CFD model with combustion shows the capability to capture both laminar and turbulent regimes. The given case illustrates that a turbulent flame develops quickly inside a mine and may transition to a detonation. This model is capable of handling detonations, so with further work an accurate model of the transition that occurs as the flame transitions from deflagration to detonation may be simulated.
- The large scale explosion simulation indicates that as the flame spreads and encounters obstacles and Gob area behind the shield, a significant pressure increase of 2.6 MPa accompanies the explosion between the shields which would be detrimental to the miners in the longwall face. The velocity and pressure contours show the model following the flame beyond the hinge supports and into the Gob immediately behind the shield hinges. The entry of the flame into the Gob indicates the success of the modeling effort.
- An ignition 2073m from the face in Gob resulted in significantly slower growth and no detonation at similar time scales as an ignition by the shields.
- The grid adaption strategy used here is the same one developed for the smaller models. That is, a relatively large mesh is used as the base grid, and grid adaption based on the methane concentration gradient is employed. This grid adaption scheme is invoked every 10-100 time steps, depending on the flame regime to ensure accuracy and coupling of the large-scale fluid dynamics effects with the small-scale chemistry.

Deliverables

The major deliverables are three manuscripts studying methane-burning velocities as a function of stoichiometry, reactor diameter, rock rubble barrier length and size, and moisture levels. The first manuscript focuses on the experiments and modeling of methane flames in various reactors of different diameters without the simulate gob. The second manuscript focuses on the development and validation of the CFD combustion model for use with simulated gob. Several vessels of various scales were used to study flame propagation through a simulate gob with various parameters to cover the various possible conditions which could be found in a longwall gob area. The third manuscript focuses on the integration of the combustion model into the large scale three dimensional CFD model of a Longwall U-type ventilation coal mine iss presented.

Fig*, M.K.; Bogin Jr.#, G.E.; Brune, J.F.; Grubb, J.W. "Experimental and numerical investigation of methane ignition and flame propagation in cylindrical tubes ranging from 5 to 71 cm – Part I: Effects of scaling from laboratory to large-scale field studies" *Journal of Loss Prevention in the Process Industries*, **Draft submitted to Journal.**

Fig*, M.K.; Bogin Jr.#, G.E.; Brune, J.F.; Grubb, J.W. "Experimental and numerical investigation of methane ignition and flame propagation in cylindrical tubes ranging from 5 to 71 cm – Part II: Effects of rock rubble from laboratory to large-scale field studies" *Journal of Loss Prevention in the Process Industries*, **Draft submitted to Journal.**

Fig*, M.K.; Bogin Jr.#, G.E.; Brune, J.F.; Grubb, J.W., Gilmore, R., " Combustion Modeling of Explosive Gas Zones in Longwall Gobs" **Draft submitted to 2016 SME Meeting**.

6.0. Conclusions and Innovation Assessment

Assessment of the innovation outcome and what impact is this expected to have on the mining health and safety

This research has resulted in several new insights with respect to methane ignition and the effects of simulated gob parameters, both experimentally and numerically. Details of these new insights were presented in section 5.0 under "Key Findings…." In summary the rock rubble increases the turbulence and pressure which results in an increase in flame propagation and shorter transition times to become fully turbulent. This is crucial as the turbulent flame can easily transition to a detonation given longer residence times and sufficient obstacles as was predicted in the fully coupled three dimensional CFD and combustion model. Preliminary results indicated rapid heating and transition to detonation where the ignition event and some EGZs were located between the shields near the edge of the rock rubble. The rock rubble just behind the shields allowed for rapid pressure build-up allowing the flame to transition from turbulent to supersonic speeds within 1 ms, the large pressure build-up as a result of the explosion would be detrimental to the workers in the longwall face. Preliminary studies with the ignition event occurring much further (2073 m from the face) in the gob area where an EGZ is located show a significantly slower growth and has not reached any detonations at similar time scales. These initial results are extremely encouraging and it is expected that with for a longer-term project a fully developed and validated model could be produced and be able to serve as a predictive model for use by mining engineers as part of mitigation strategies to increase the safety of mine workers.

Justification and recommendations for expanding promising results from exploratory work

Significant progress was made over the 15 month short-term exploratory project considering that several flame reactors were built ranging in size from 5 cm to 71cm in diameter and 1.2 m to 6.1 m in length, resulting in a wide range of experiments performed to assess the impact of various gob conditions could have on methane flame propagation. This was done in parallel with the development and validation of a combustion model capable of simulating flame propagation with a simulated gob and finally resulted in the integration of that model into a three-dimensional CFD model of a Longwall Coal mine. The accomplishments and insights provided in this short-term project provided some interesting observations especially for rich methane-air mixtures and size of rocks in the rubble that will require additional investigation. Along with these observations were some promising results from the full-scale model which was previously only able to predict EGZs, now has the ability to model methane explosions. Expanding this research can have a huge impact on the mining industry providing for the first time a full-scale model capable of predicting the explosion hazards on mine workers under various ventilation schemes and possibly generating new ideas for mitigation strategies.

Short synopsis and proposed additional research

The potential for future research built off the successes described above include:

1) The potential to perform experimental and modeling assessments of inert injection strategies. The explosion pressure flame reactor is equipped with more than enough ports to allow a broad range of gas or vapor injections along the axis. Such additions to the model would not be overly difficult.

2) The possibility to perform experimental and modeling assessments of the effects of coal-dust entrainment into a propagating flame. The existence of coal and rock dust through both the active face and Gob areas virtually guarantee this needs to be taken into account in any realistic approach. This is thought to be a major contributor to the explosive violence in real explosions. As the explosion pressure flame reactor is capable of handling high pressures such as found in detonations, this kind of work could be done with this equipment. Another proposed idea is to use a larger quartz reactor similar to the one used in this research to visualize the entrainment of coal dust after a methane-air mixture has been ignited. It is believed that being able to capture this will provide great insight into the dynamics of a methane-coal dust gas explosion and would allow the development of combustion mining models which are capable of capturing these key features providing additional strategies for mitigation and/or minimization of these potential hazards a longwall coal mine.

Funding from the Alpha Foundation for the Improvement of Mine Safety and Health has allowed the successful development and validation of a CFD combustion model for studying methane flames in a simulated gob environment and the final integration of the combustion model with a three dimensional CFD model of a Longwall coal mine with U-type ventilation scheme which is currently able to predict the impact of a methane explosion. These results should prove useful in the continued drive toward higher standards of miner safety.

7.0 References

1. Brune J.F. The Methane-Air Explosion Hazard Within Coal Mine Gobs, SME Transactions, Vol. 334, October 2013.

2. McKinney R, Crocco W, Tortorea JS, Wirth GJ, Weaver CA, Urosek JE, Beiter DA, Stephan CR [2001]. Report of investigation, underground coal mine explosions, July 31–August 1, 2000. Willow Creek mine, MSHA ID No. 42–02113, Plateau Mining Corporation, Helper, Carbon County, Utah.

3. Page NG et al.,Report of Investigation, Fatal Underground Mine Explosion, April 5, 2010, Upper Big Branch Mine-South, Performance Coal Company, Montcoal, Raleigh County, West Virginia, ID No. 46-08436, Mine Safety and Health Administration, Arlington, Virginia, 2011, 965p.

4. Balusu, R., Tuffs, N., Peace, R., and Xue, S., (2005), "Longwall Goaf Gas Drainage and Control Strategies for Highly Gassy Mines", 8th International Mine Ventilation Congress.

5. Yuan, L., and Smith, A.C., (2010), "Effect of Longwall Face Advance on Spontaneous Heating in Longwall Gob Area", *Mining Engineering,* Vol. 62, No. 3, pp. 2-6

6. Ren, T., Wang, Z., Nemcik, J., Aziz, N., and Wu, J., (2012), "Investigation of Spontaneous Heating Zones and Proactive Inertisation of Longwall Goaf in Fenguangshan Mine", *12th Coal Operators' Conference*

7. Ren, T.X., Balusu, R., and Humphries, P., (2005), "Development of Innovative Goaf Inertisation Practices to Improve Coal Mine Safety", *Coal Operators' Conference*

8. Ren, T.X., and Balusu, R., (2009), "Proactive Goaf Inertisation for Controlling Longwall Goaf Heatings", *Procedia Earth and Planetary Science,* Vol. 1, No. 1, pp. 309-315

9. Ren, T., Balusu, R., and Claassen, C., (2011), "Computational Fluid Dynamics Modelling of Gas Flow Dynamics in Large Longwall Goaf Areas", *35th APCOM Symp. - Application of Computers and Operations Res. in the Miner. Industry,* pp. 603-613

10. Ren, T.X., and Balusu, R., (2008), "Investigation of Heatings and Related CO and H2 Gas Flow Patterns in Longwall Goafs", *CSIRO Explor. and Mining Report P2008/2299*

11. Yuan, L., and Smith, A.C., (2008), "Numerical Study on Effects of Coal Properties on Spontaneous Heating in Longwall Gob Areas", *Fuel,* Vol. 87, pp. 3409-3419

12. Mihalik, T.A.; Lee, J.H.S. The Flammability limits of gaseous mixtures in porous media,

13. Bulgakov, Y.F. Experimental investigation of explosion-suppression properties of gob rocks under laboratory and mine conditions, Procedia Earth and Planetary Science I, pgs. 199-202, 2009

14. Howell, J.R.; Hall, M.J.; Ellzey, J.L. Combustion of hydrocarbon fuels within porous inert media, Prog. Energy Combust Sci. Vol. 22, pp. 121-145, 1996,

15. Gilmore, R.C., Marts, J.A., Brune, J.F., Worrall, D.M. (Jr.), Bogin, G.E. (Jr.), and Grubb, J.W., (2013), "Control of Explosive Zones in Longwall Gobs Through Nitrogen Injection", 23rd World Mining Congress

16. Marts, J., Brune, J., Gilmore, R., Worrall, D., and Grubb, J., (2013), "Impact of Face Ventilation and Nitrogen Inertization on Hazardous Gas Distribution in Bleederless Longwall Gobs", Mining Engineering, Vol. 65, No. 9, pp. 71-77

17. Marts, J.A., Gilmore, R.C., Brune, J.F., Bogin, G.E. Jr., Grubb, J.W., (2014), "Dynamic Gob Response and Reservoir Properties for Active Longwall Coal Mines", 16th Annual North American Ventilation Conference, Salt Lake City UT

18. ANSYS, Inc. Release 14, Ansys FLUENT, 2012.

19. Itasca Consulting Group, Inc., Fast Langrage Analysis of Continua in Three Dimensions (FLAC®), Itasca Consulting Group, Inc., 2009.

20. Sapko, M.J.; Weiss, E.S. Evaluation of New Methods and Facilities to Test Explosion Resistant Seals, Proceedings of the 29th International Conference on Safety in Mines Research Institute, October 8 -11, Katowice, Poland, pp. 157 – 166.

21. http://www.ANSYS.com/Products/ANSYS+15.0+Release+Highlights/Fluids

22. Marts*, J.; Gilmore*, R.; Brune, J.; **Bogin, G.;** Grubb, J.; Saki*, S. Accumulations of Explosive Gases in Longwall Gobs and Mitigation through Nitrogen Injection and Face Ventilation Method. 6th Aachen International Mining Symposia (AIMS), Aachen, Germany, **2014**, p. 347 – 358

8.0 Appendices

9.0 Acknowledgements/Disclaimer

The research participants would like to thank the Alpha foundation for funding this interesting and challenging research. We would also like to thank the Edgar Mine for hosting the larger test facility and for assistance provided throughout installation and testing.

Disclaimer: